

Supporting Information

**Internal Heavy-Atom Effect in 3-Phenylselanyl and 3-Phenyltellanyl BODIPY  
Derivatives Studied by Transient Absorption Spectroscopy**

*Jamaludin Al Anshori, Tomáš Slanina, Eduardo Palao, Petr Klán\**

*RECETOX, Faculty of Science, Masaryk University, Kamenice 5, 625 00, Brno*

\* E-mail: klan@sci.muni.cz; Phone: +420-54949-4856; Fax: +420-54949-2443

**Table of Contents**

Spectra, irradiation experiments, solvent and concentration dependences	S2
Transient absorption spectra	S7
UV-vis, fluorescence and excitation spectra of <b>1–5, and 8</b>	S16
HPLC chromatogram of photoproduct of <b>2</b> spiked by internal standard	S22
NMR spectra	S23
Determination of the ISC quantum yield	S31
Light Saturation Test	S35
Determination of the ISC Quantum Yield by a Reference Method	S39
References	S41

**Figure S1:** UV-vis spectra of **1** in acetonitrile (black line) and in a water/acetonitrile mixture (99:1; v/v, red line);  $c \sim 1 \times 10^{-5} \text{ mol dm}^{-3}$ .

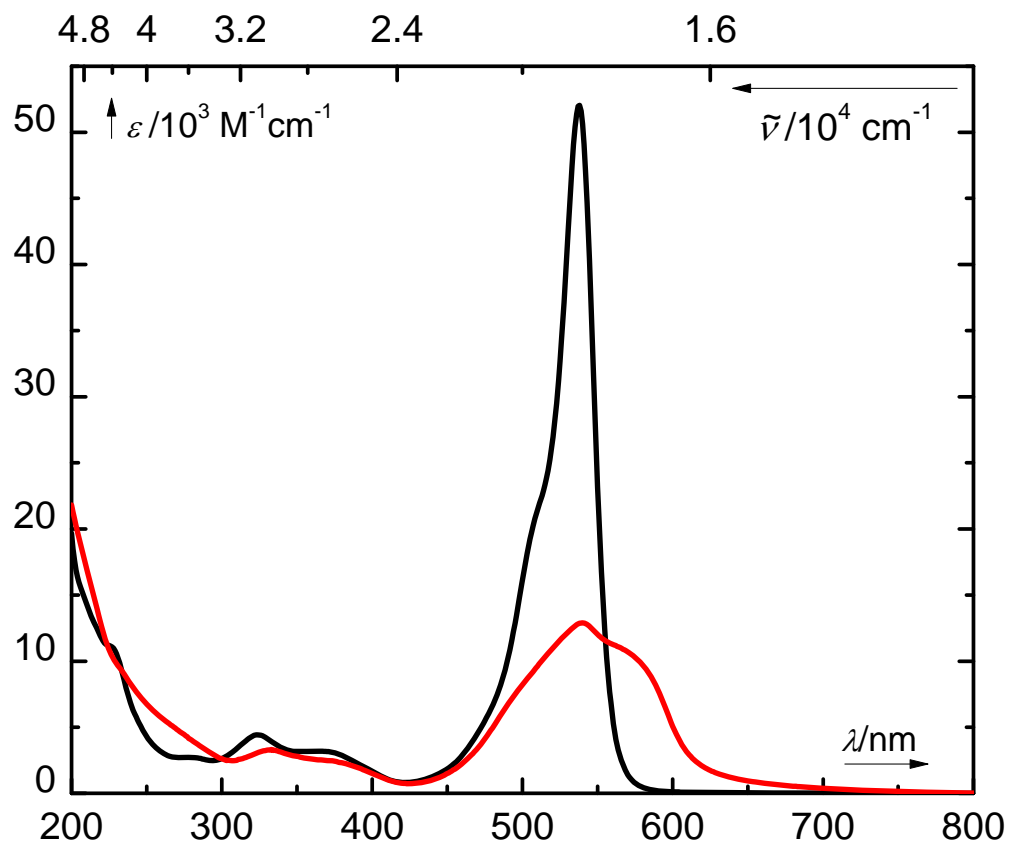


**Figure S2:** Dependence of the absorption spectrum of **2** in acetonitrile ( $c = \sim 1 \times 10^{-6} \text{ mol dm}^{-3}$  to  $\sim 1 \times 10^{-4} \text{ mol dm}^{-3}$ ) measured in a 10.0 mm cuvette; the spectrum at  $c = \sim 4 \times 10^{-4} \text{ mol dm}^{-3}$  measured in a 1.0 mm cuvette is shown as an orange thick line.

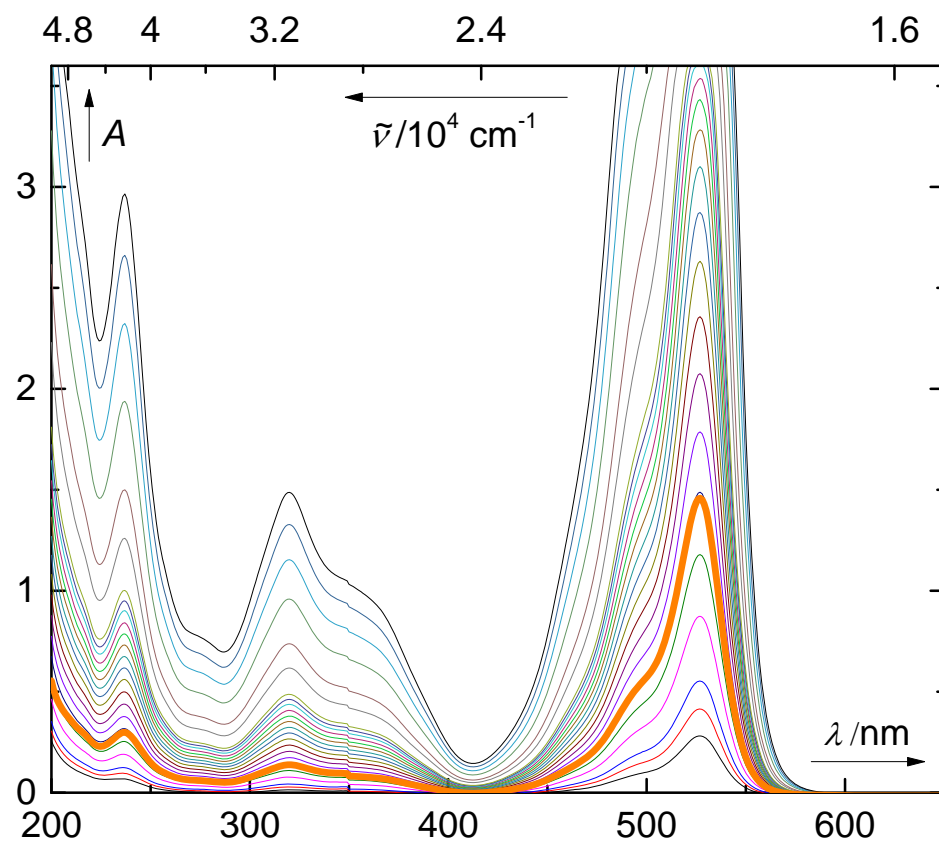


**Figure S3:** Irradiation of **1** in acetonitrile ( $c = 2.3 \times 10^{-5} \text{ mol dm}^{-3}$ ) at 525 nm; the spectra were taken every 60 min.

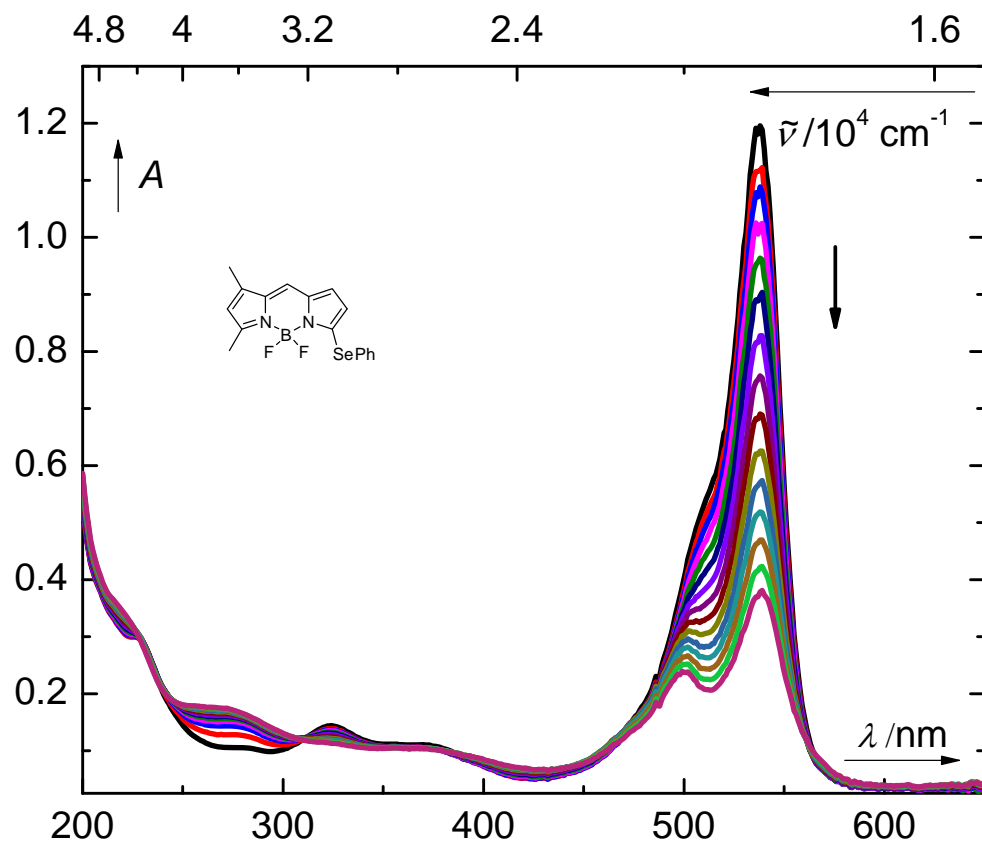


**Figure S4:** Irradiation of **2** in acetonitrile ( $c = 2.9 \times 10^{-5} \text{ mol dm}^{-3}$ ) at 525nm; the spectra taken every 150 min.

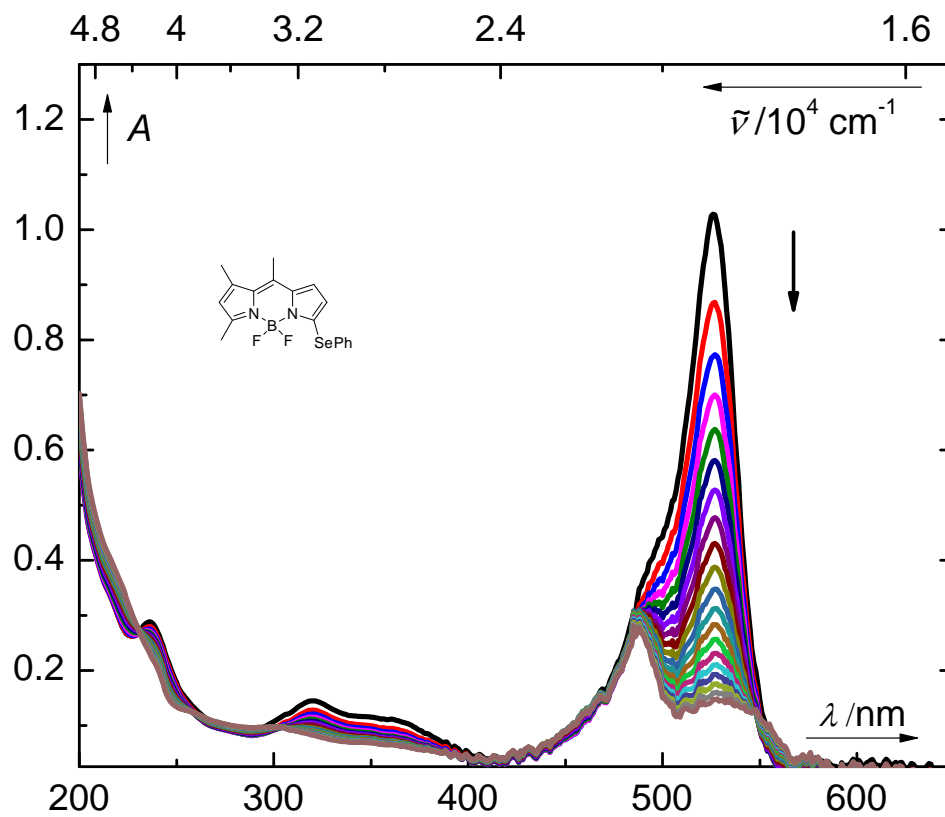


**Figure S5:** Irradiation of **3** in acetonitrile ( $c = 2.6 \times 10^{-5} \text{ mol dm}^{-3}$ ) at 525nm; the spectra taken every 30 s; an initial spectrum (black line), a final spectrum (red line).

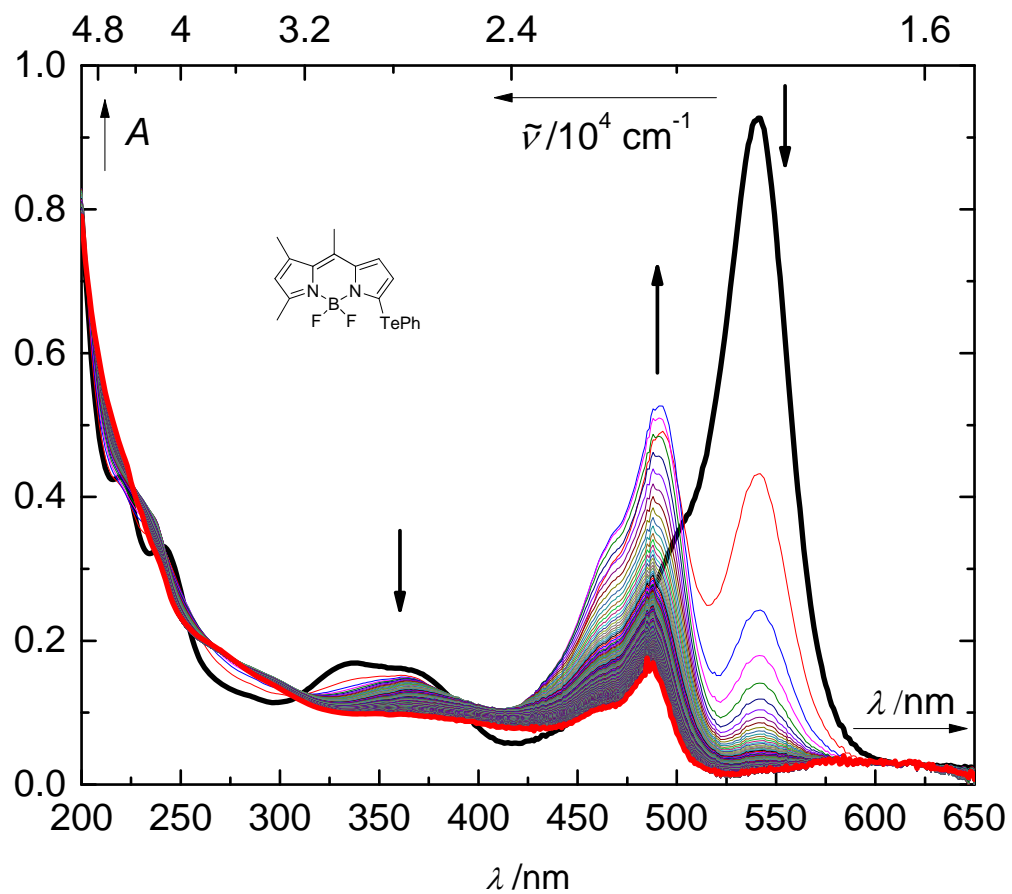


**Figure S6:** Transient spectra of **1** in degassed acetonitrile ( $c = 1.10 \times 10^{-5} \text{ mol dm}^{-3}$ ) taken at different times after excitation;  $\lambda_{\text{exc}} = 532 \text{ nm}$

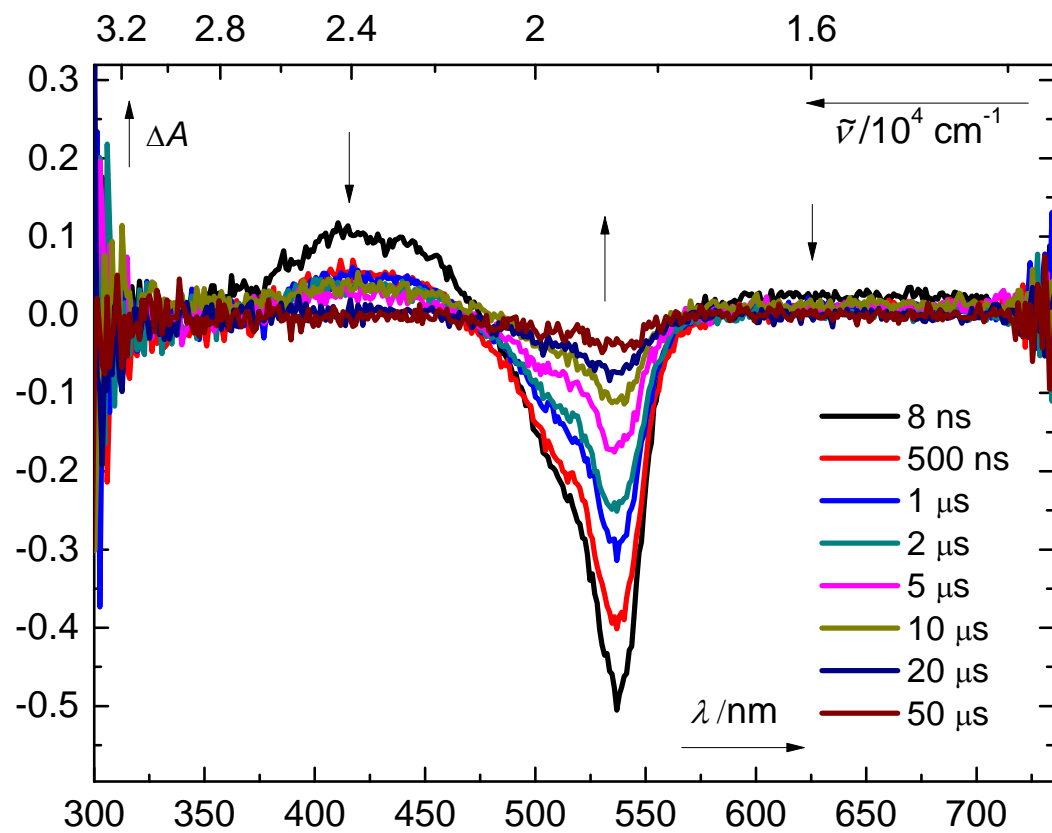


**Figure S7:** Transient spectra of **2** in non-degassed acetonitrile ( $c = 1.46 \times 10^{-5} \text{ mol dm}^{-3}$ ) taken at different times after excitation;  $\lambda_{\text{exc}} = 532 \text{ nm}$

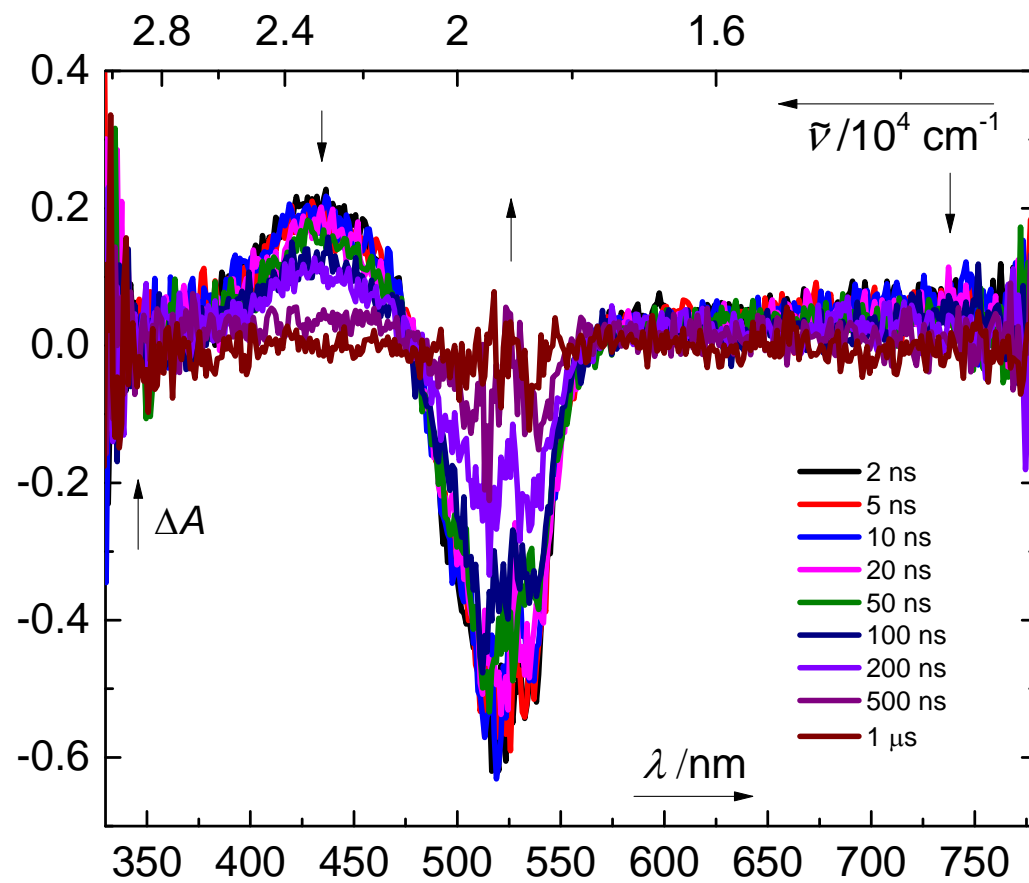


**Figure S8:** Transient spectra of **2** in degassed acetonitrile ( $c = 1.46 \times 10^{-5} \text{ mol dm}^{-3}$ ) taken at different times after excitation;  $\lambda_{\text{exc}} = 532 \text{ nm}$

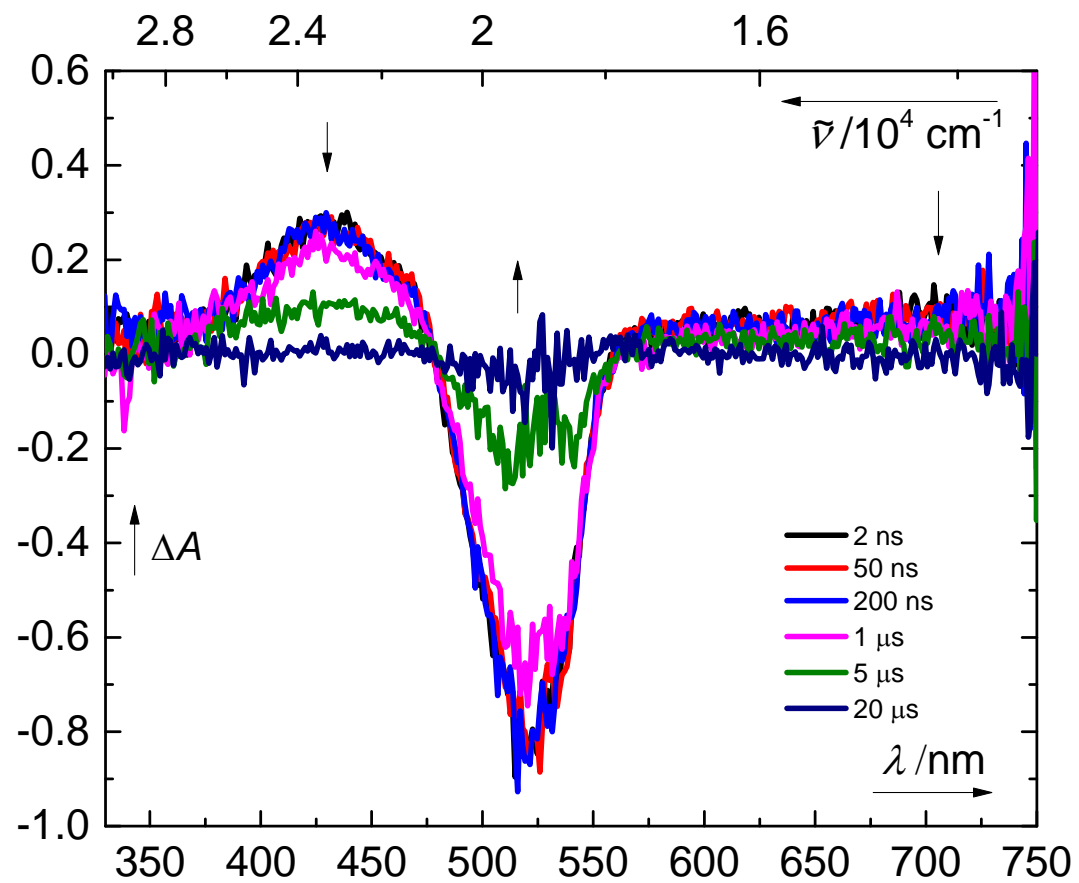


**Figure S9:** Transient spectra of **3** in non-degassed acetonitrile ( $c = 1.55 \times 10^{-5} \text{ mol dm}^{-3}$ ) taken at different times after excitation;  $\lambda_{\text{exc}} = 532 \text{ nm}$

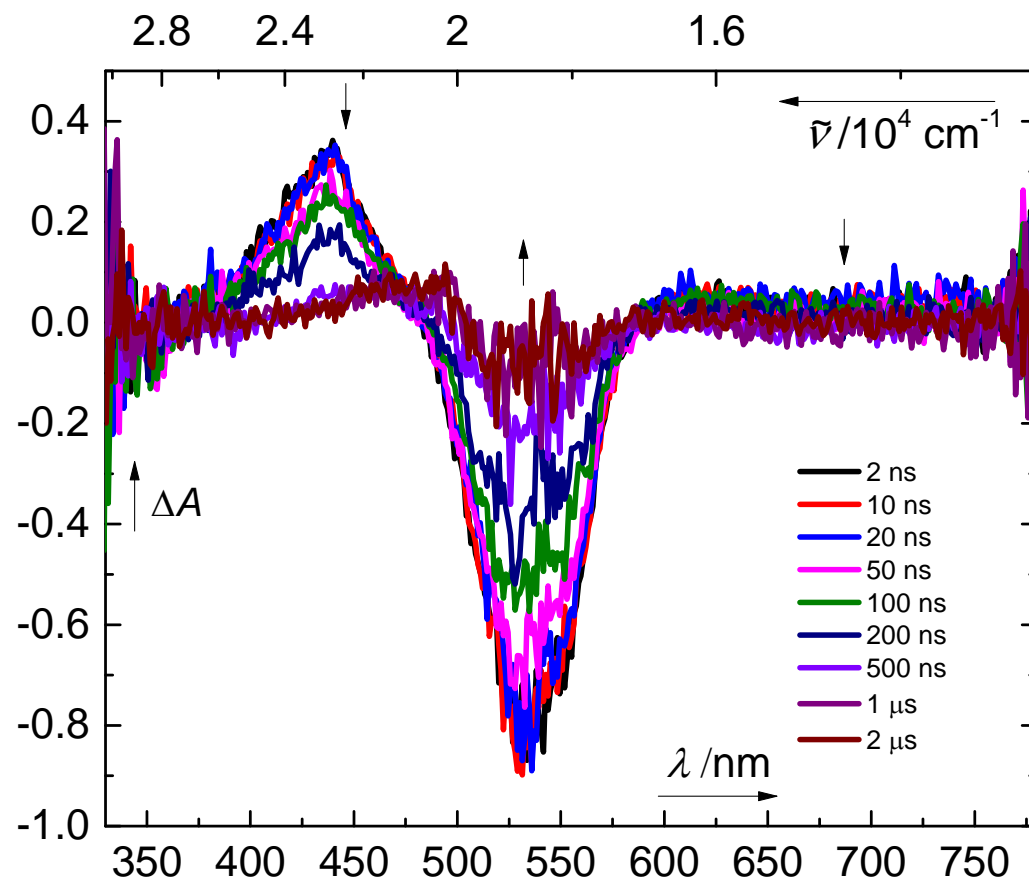


**Figure S10:** Transient spectra of **3** in degassed acetonitrile ( $c = 1.55 \times 10^{-5} \text{ mol dm}^{-3}$ ) taken at different times after excitation;  $\lambda_{\text{exc}} = 532 \text{ nm}$

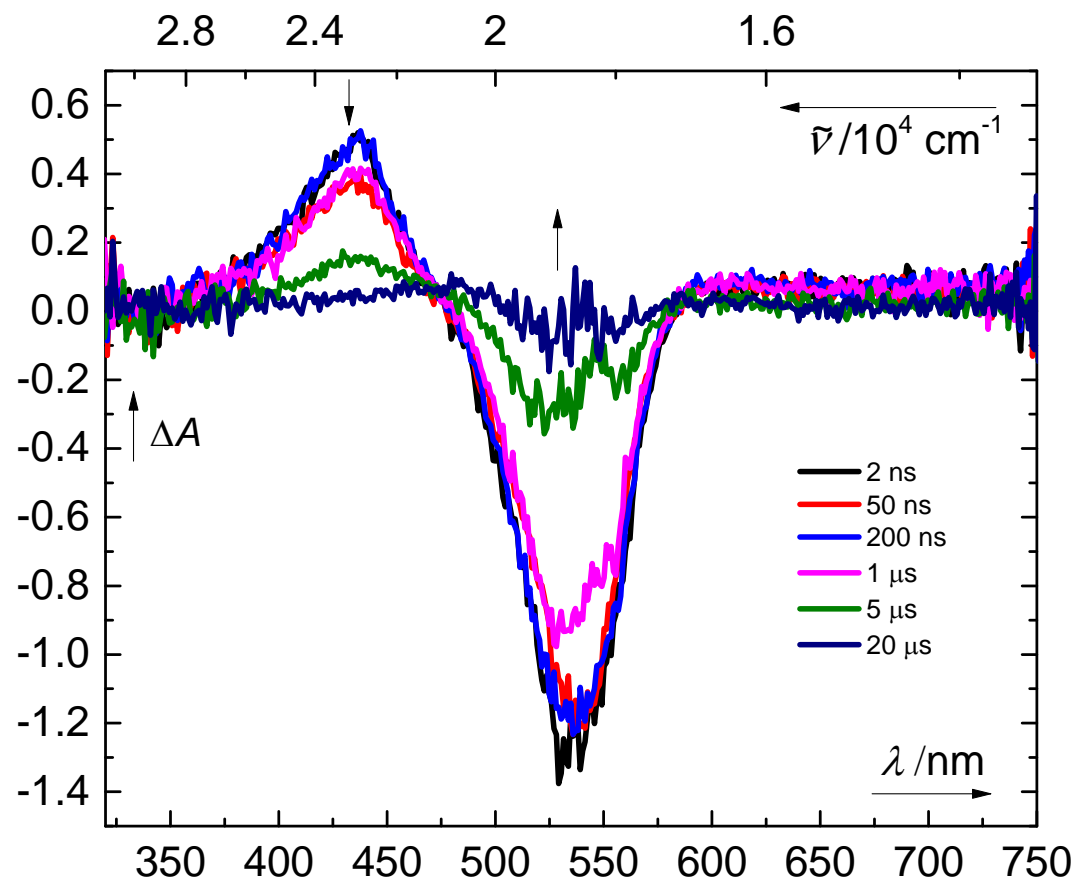


**Figure S11:** Transient spectra of **4** in non-degassed acetonitrile ( $c = 4.42 \times 10^{-5} \text{ mol dm}^{-3}$ ) taken at different times after excitation;  $\lambda_{\text{exc}} = 355 \text{ nm}$

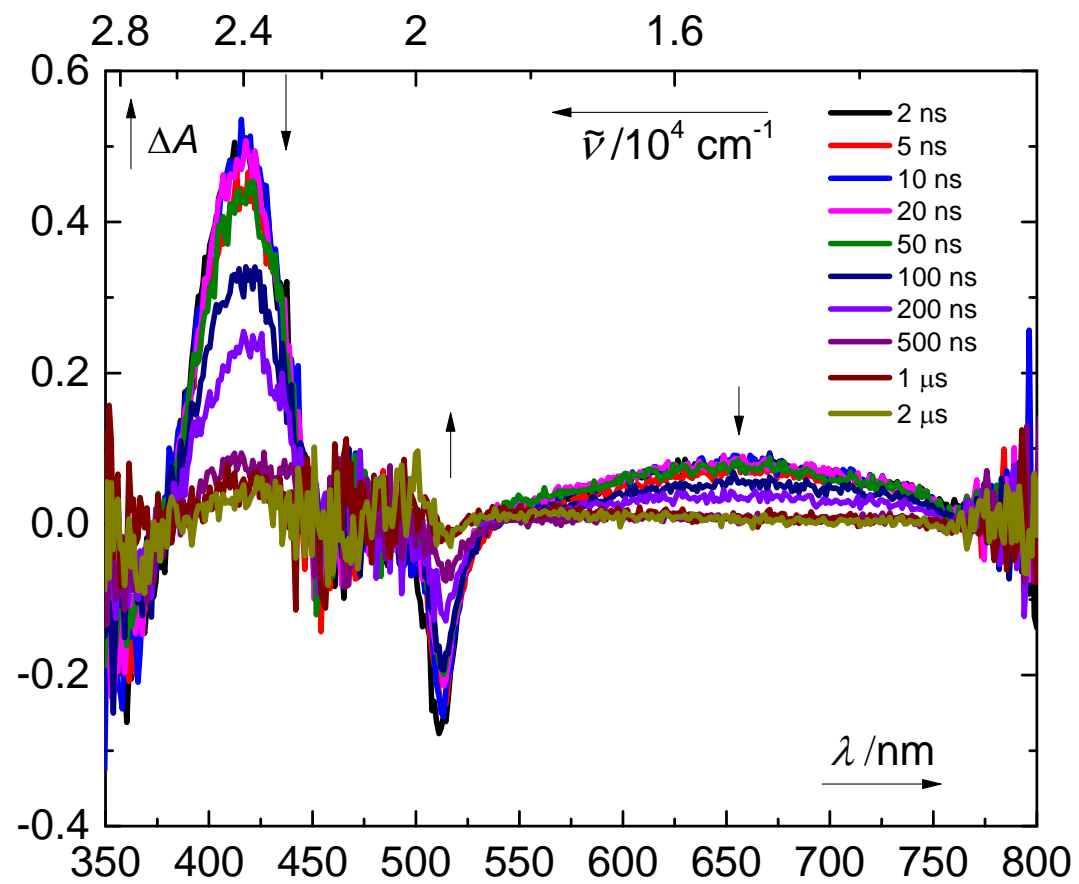


**Figure S12:** Transient spectra of **4** in degassed acetonitrile ( $c = 4.42 \times 10^{-5} \text{ mol dm}^{-3}$ ) taken at different times after excitation;  $\lambda_{\text{exc}} = 355 \text{ nm}$

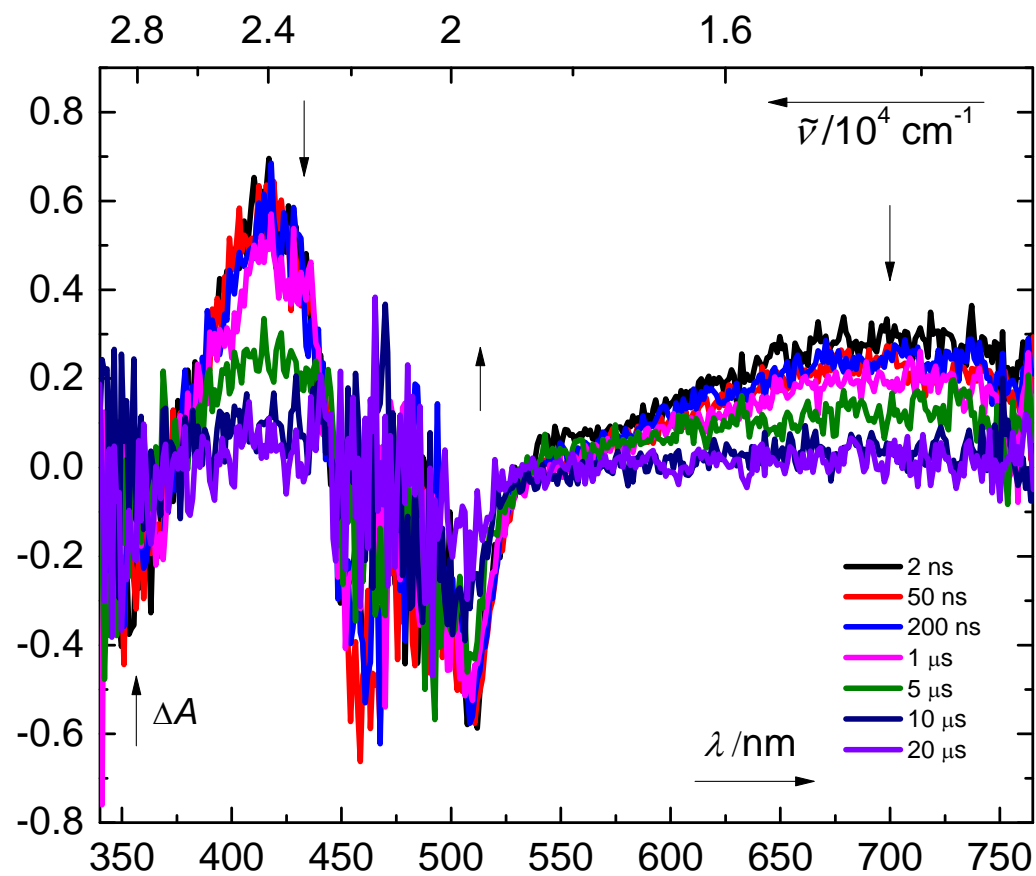


**Figure S13:** Transient spectrum of **7** in non-degassed acetonitrile ( $c = 1.00 \times 10^{-4} \text{ mol dm}^{-3}$ ) taken at 2 ns after excitation;  $\lambda_{\text{exc}} = 355 \text{ nm}$

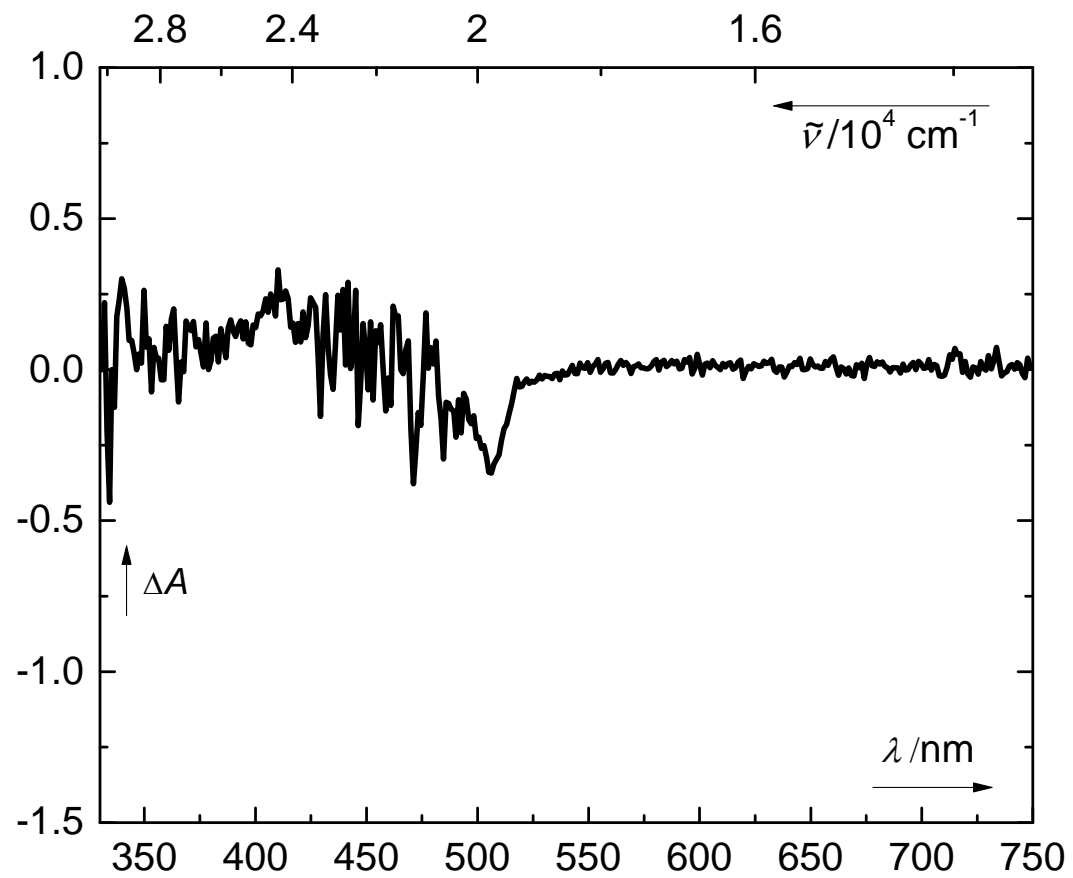


**Figure S14.** Transient spectra ( $\lambda_{\text{exc}} = 532 \text{ nm}$ ) of **1–4** in aerated acetonitrile solutions obtained 2 ns after the excitation (the molar absorption coefficients are shown; **1**: light green; **2**: orange; **3**: dark green; **4**: magenta).

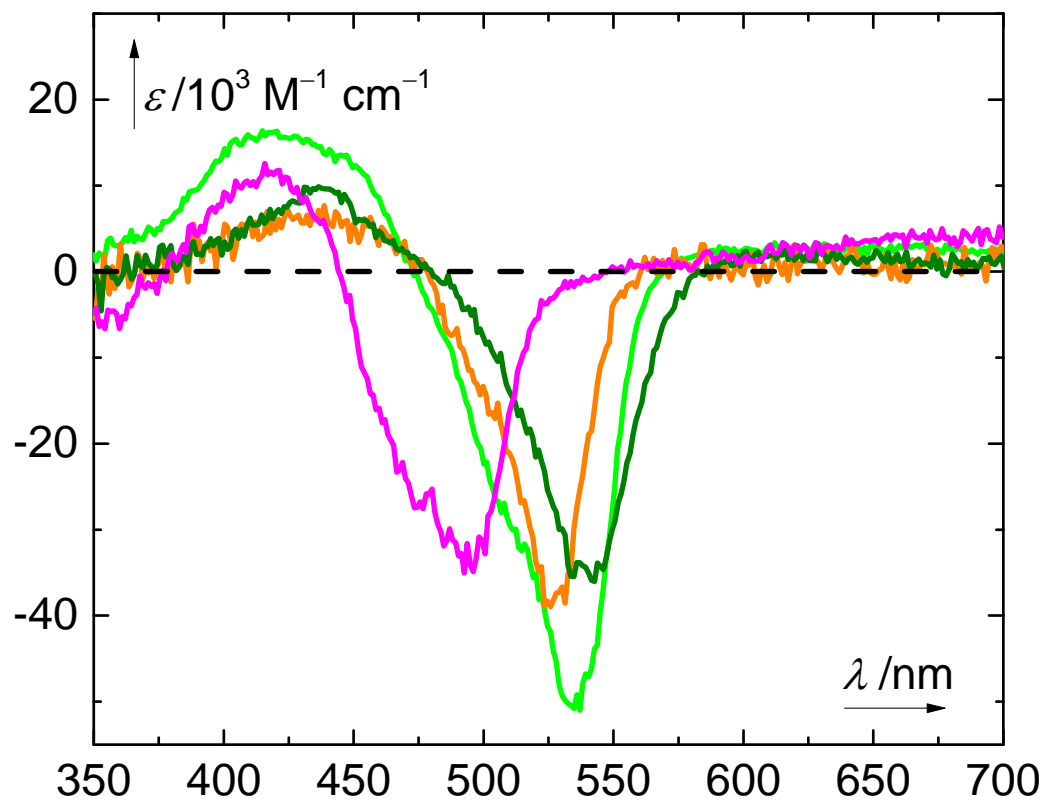


**Figure S15:** Absorption (solid black line; left ordinate), emission ( $\lambda_{\text{ex}} = 450 \text{ nm}$ ; solid orange line, normalized; right ordinate) and excitation ( $\lambda_{\text{em}} = 565 \text{ nm}$ ; dashed blue line, normalized; right ordinate) spectra of **1** in acetonitrile ( $c \sim 1 \times 10^{-5} \text{ mol dm}^{-3}$ )

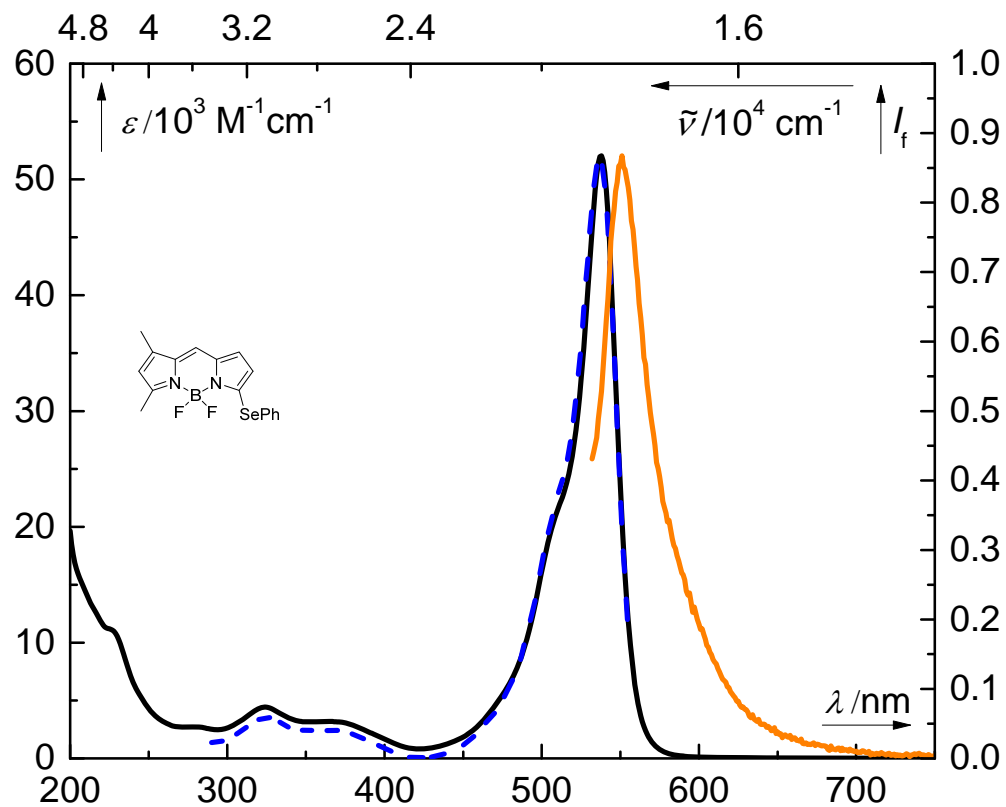


**Figure S16:** Absorption (solid black line; left ordinate), emission ( $\lambda_{\text{ex}} = 450 \text{ nm}$ ; solid orange line, normalized; right ordinate) and excitation ( $\lambda_{\text{em}} = 558 \text{ nm}$ ; dashed blue line, normalized; right ordinate) spectra of **2** in acetonitrile ( $c \sim 1 \times 10^{-5} \text{ mol dm}^{-3}$ )

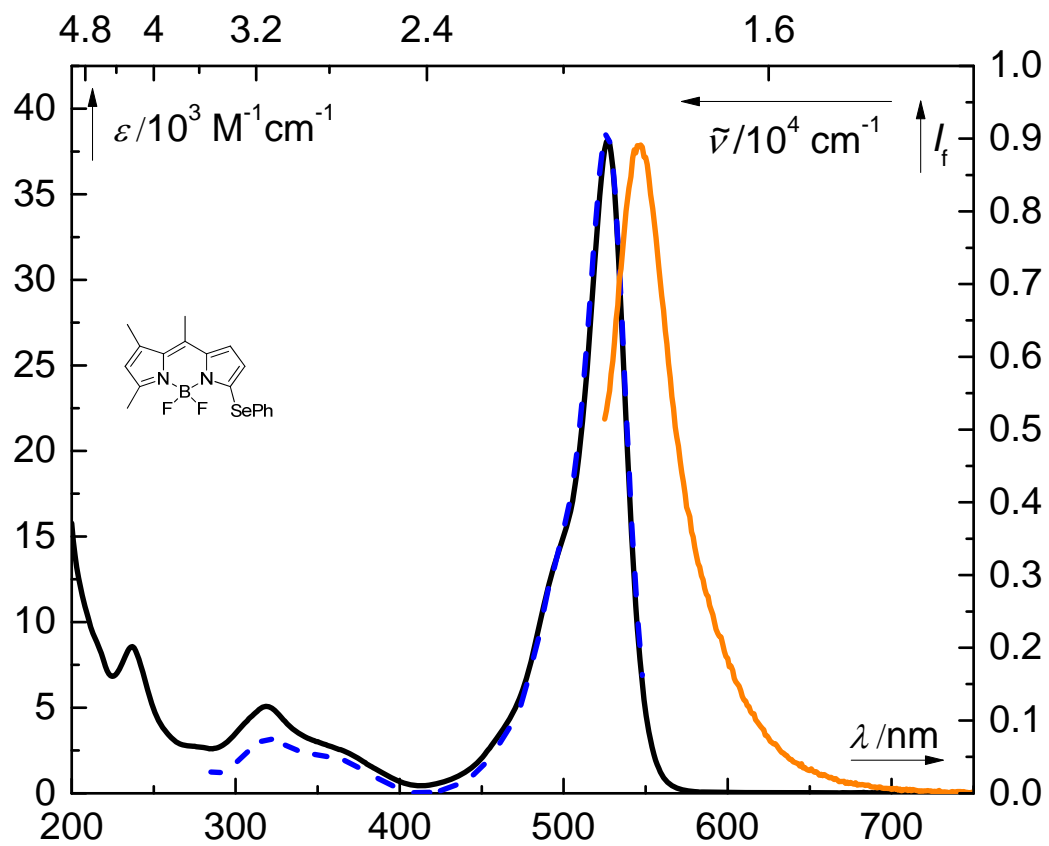


**Figure S17:** Absorption (solid black line, shown in molar absorption values; left ordinate), emission ( $\lambda_{\text{ex}} = 540 \text{ nm}$ ; solid orange line, normalized; right ordinate) and excitation ( $\lambda_{\text{em}} = 585 \text{ nm}$ ; dashed blue line, normalized; right ordinate) spectra of **3** in acetonitrile ( $c \sim 1 \times 10^{-5} \text{ mol dm}^{-3}$ ); the band at 490 nm in the excitation spectrum corresponds to contamination by **5** formed upon irradiation by fluorimeter excitation light

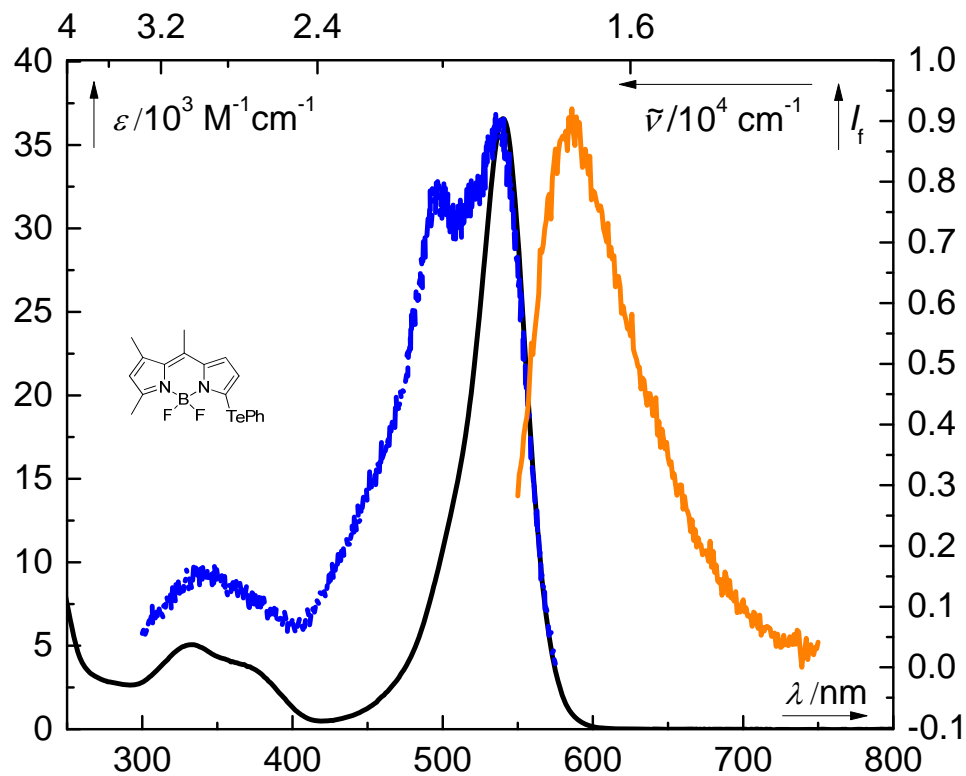


**Figure S18:** Absorption (solid black line, shown in molar absorption values; left ordinate), emission ( $\lambda_{\text{ex}} = 460$  nm; solid orange line, normalized; right ordinate) and excitation ( $\lambda_{\text{em}} = 532$  nm; dashed blue line, normalized; right ordinate) spectra of **4** in acetonitrile ( $c \sim 1 \times 10^{-5}$  mol dm $^{-3}$ )

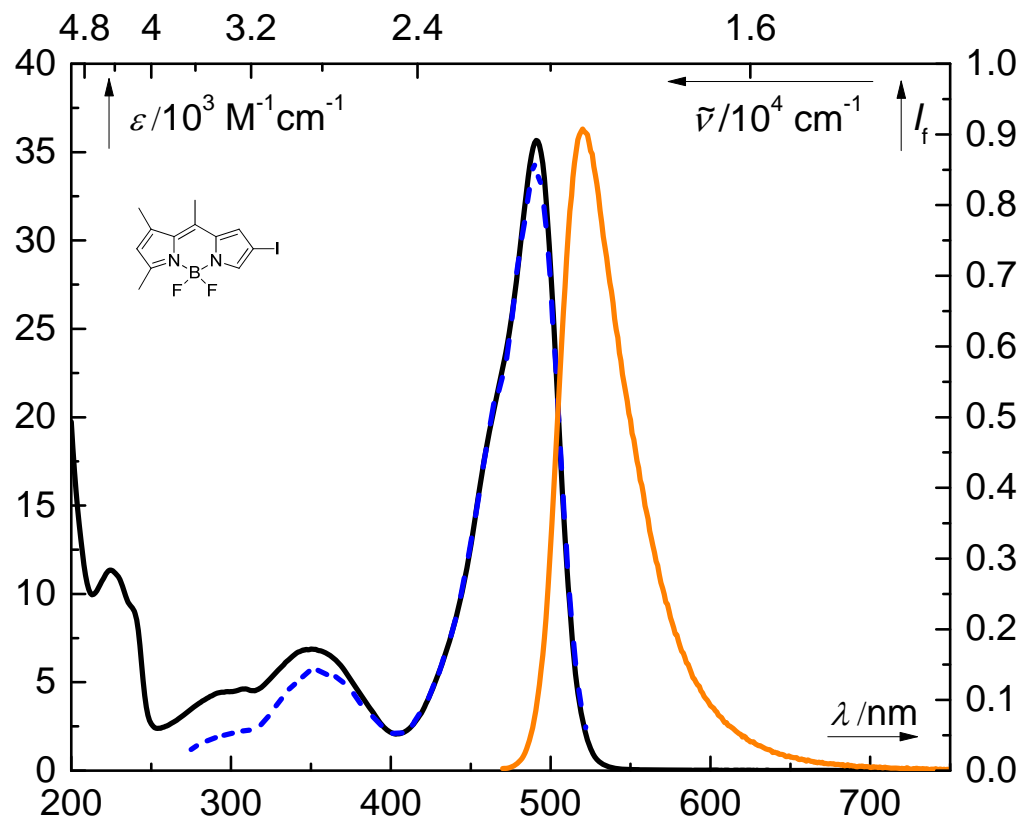


**Figure S19:** Absorption (solid black line, shown in molar absorption values; left ordinate), emission ( $\lambda_{\text{ex}} = 440 \text{ nm}$ ; solid orange line, normalized; right ordinate) and excitation ( $\lambda_{\text{em}} = 525 \text{ nm}$ ; dashed blue line, normalized; right ordinate) spectra of **5** in acetonitrile ( $c \sim 1 \times 10^{-5} \text{ mol dm}^{-3}$ )

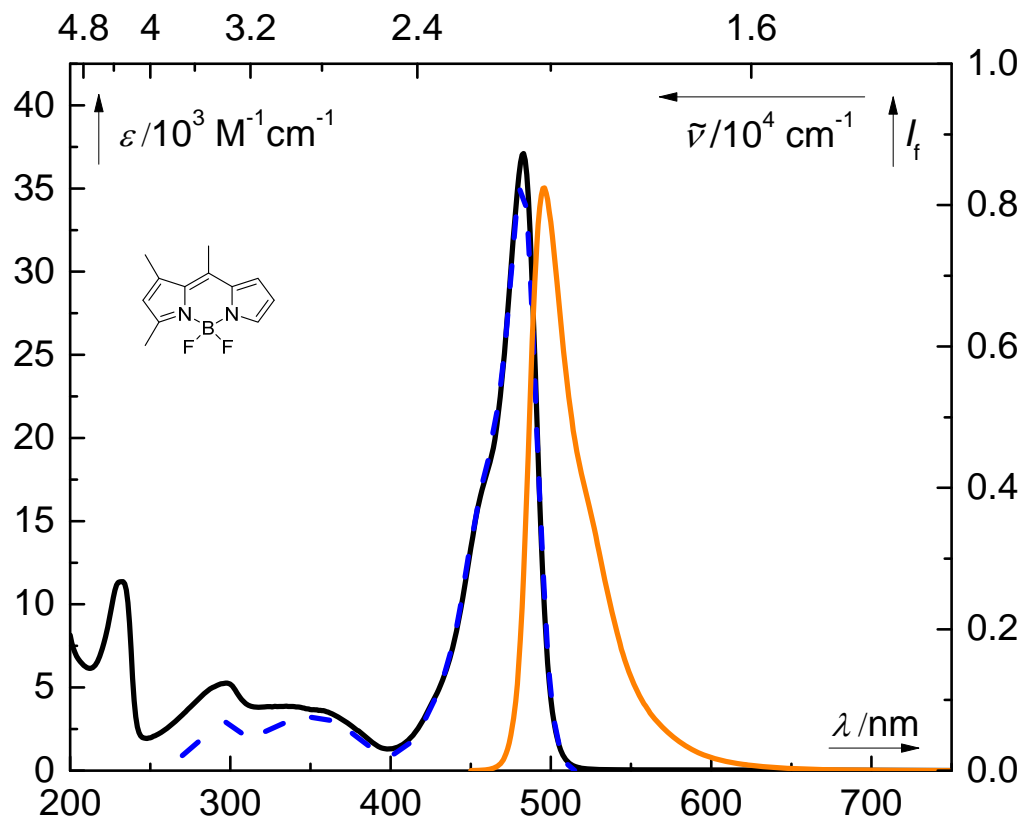


**Figure S20.** Normalized absorption and emission spectra of the photoproduct (**8**) formed from the compound **1** upon irradiation: A solution of **1** ( $c \sim 3.65 \times 10^{-6} \text{ mol dm}^{-3}$ ) in  $\text{CHCl}_3$  was irradiated using high-energy LEDs (100 mW;  $545 \pm 15 \text{ nm}$ ) at the distance of  $\sim 1 \text{ cm}$  from the cuvette window. The absorption spectra were treated with a Levenberg-Marquardt method and compared to the reported ones.<sup>1</sup>

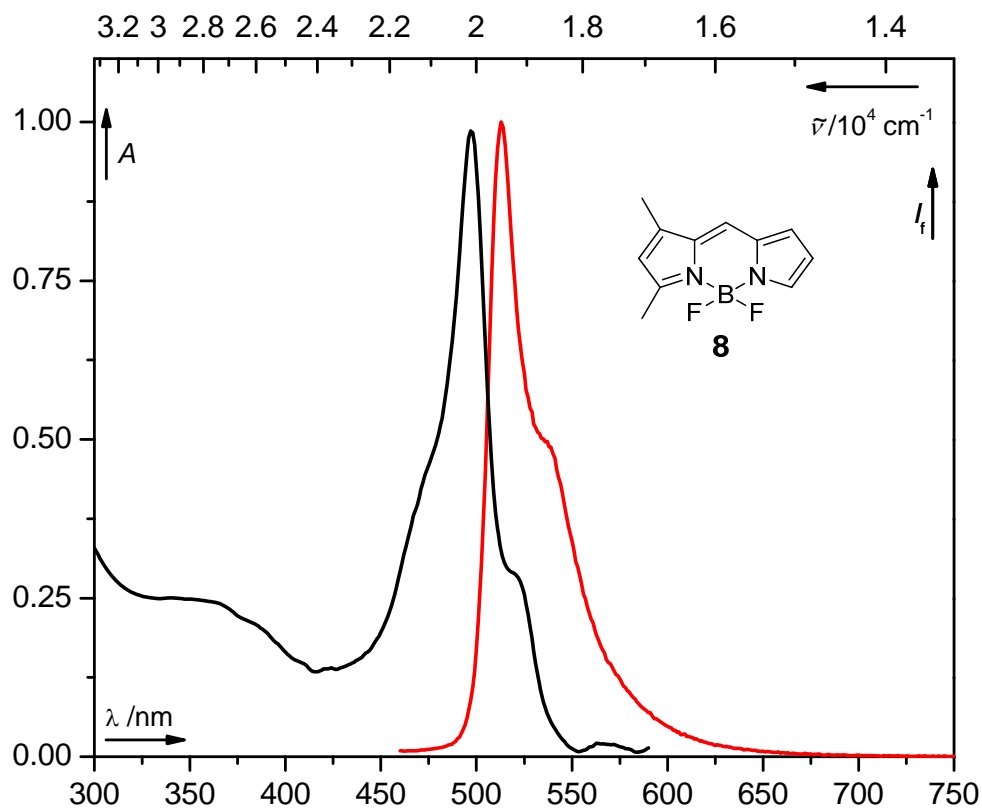


**Figure S21.** Irradiation of the compound **2** ( $c \sim 1 \times 10^{-6}$  mol dm<sup>-3</sup> in an acetonitrile solution) using high-energy LEDs (100 mW;  $\lambda_{em} = 525.5$  nm) at the distance of  $\sim 1$  cm from the cuvette window: The photoproduct (**5**) was identified by HPLC (acetonitrile 0.1 mL/min; C-8 column; DAD  $\lambda_{detection} = 488$  nm; FLD  $\lambda_{exc} = 460$  nm;  $\lambda_{em} = 497$  nm) using an internal standard.

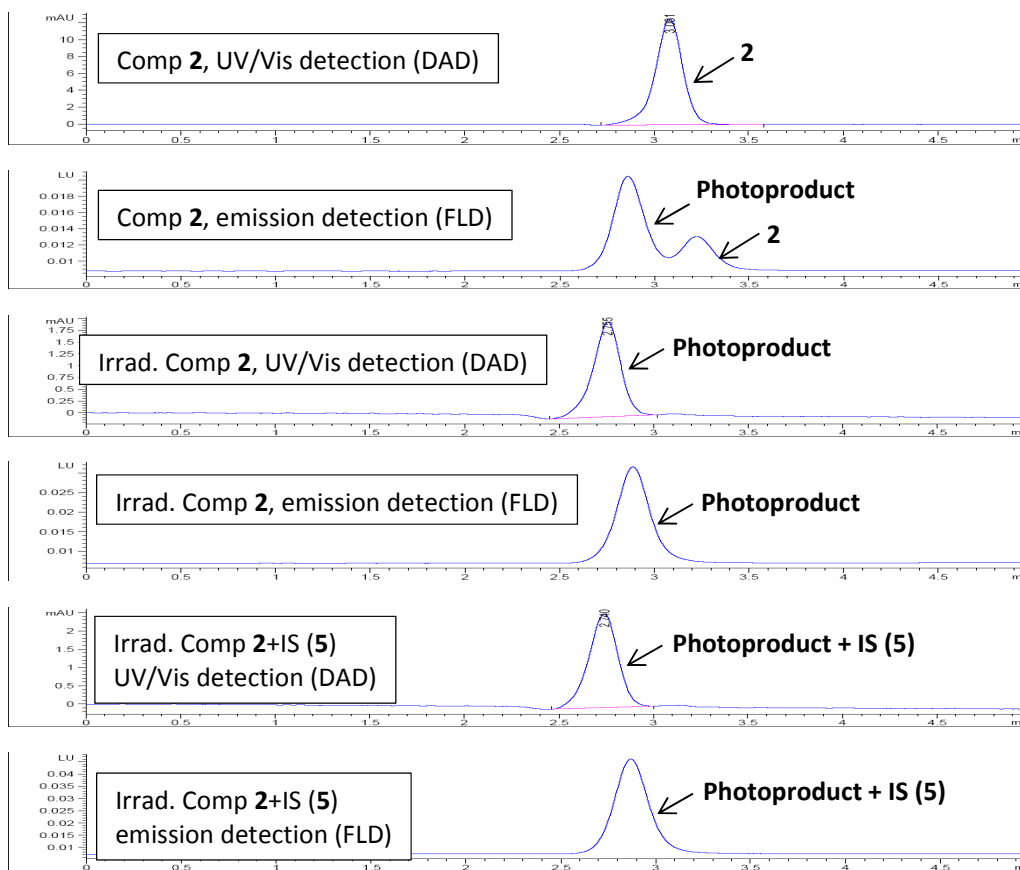


**Figure S22:**  $^1\text{H-NMR}$  of 3-phenylselanyl-4,4-difluoro-5,7-dimethyl-4-bora-3a,4a-diaza-*s*-indacene (**1**) in dichloromethane- $d_2$

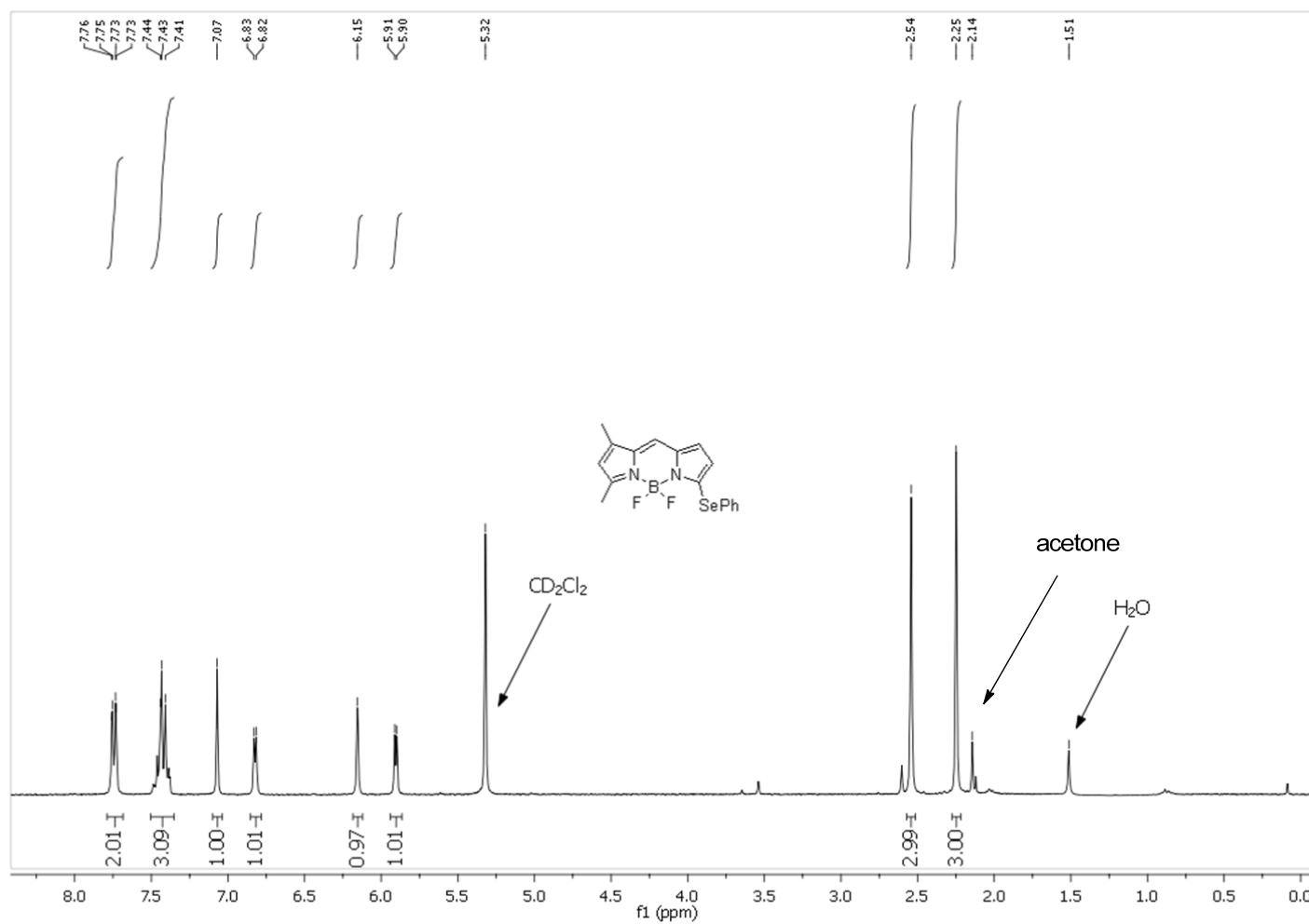


Figure S23:  $^{13}\text{C}$ -NMR of 3-phenylselanyl-4,4-difluoro-5,7-dimethyl-4-bora-3a,4a-diaza-s-indacene (**1**) in dichloromethane- $d_2$

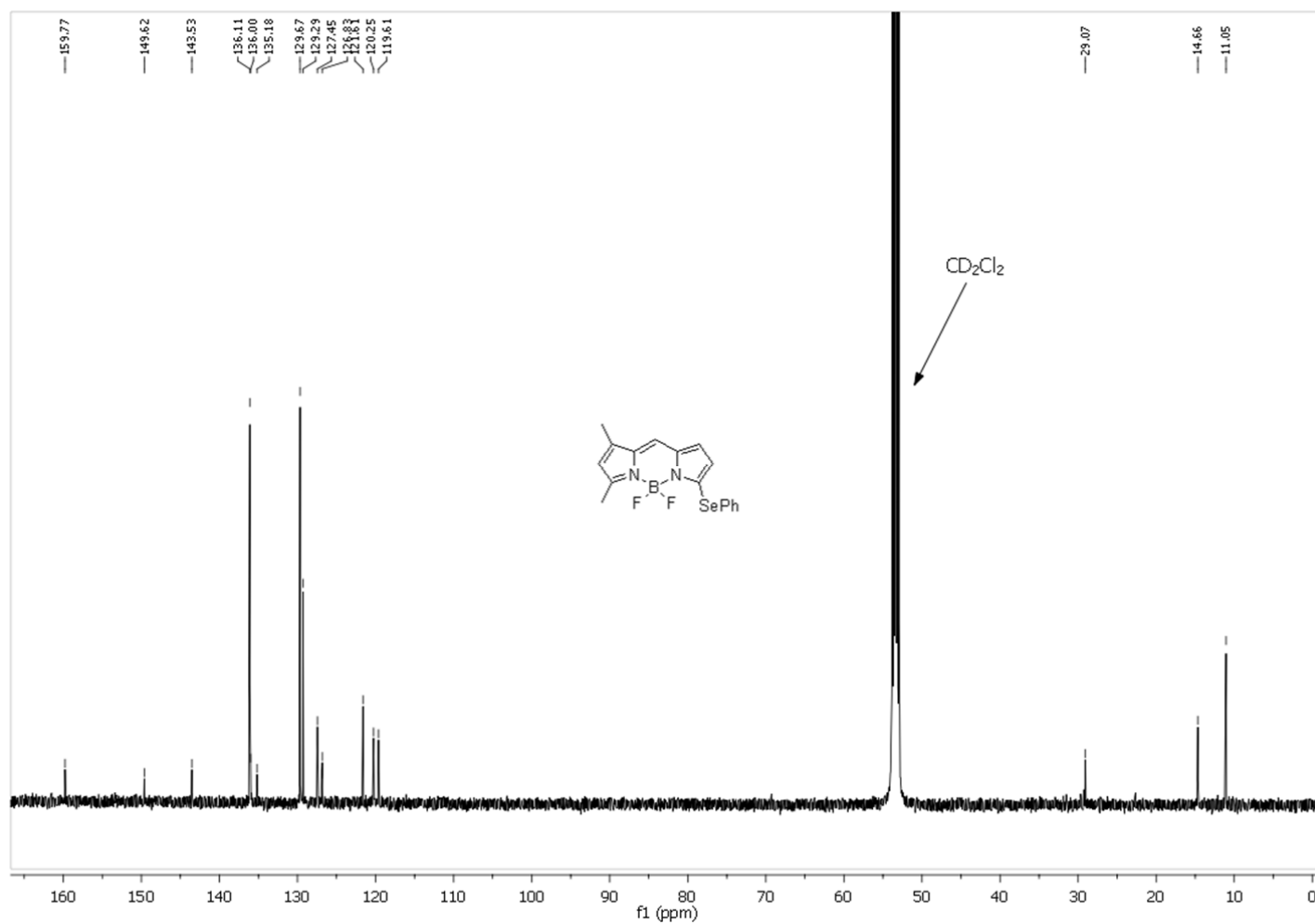


Figure S24:  $^1\text{H-NMR}$  of 3-phenylselanyl-4,4-difluoro-5,7,8-trimethyl-4-bora-3a,4a-diaza-s-indacene (**2**) in dichloromethane- $d_2$

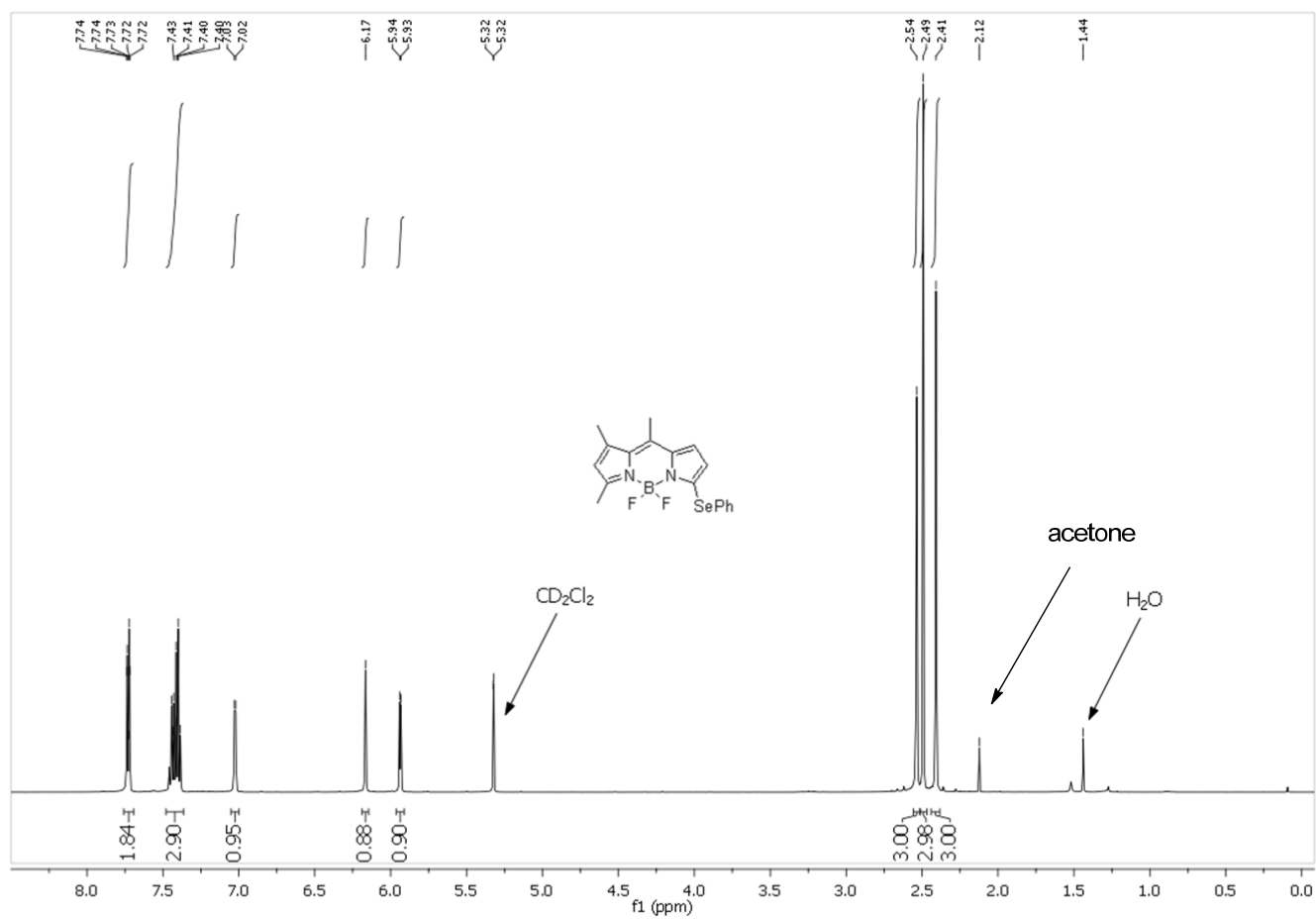


Figure S25:  $^{13}\text{C}$ -NMR of 3-phenylselanyl-4,4-difluoro-5,7,8-trimethyl-4-bora-3a,4a-diaza-*s*-indacene (**2**) in dichloromethane- $d_2$

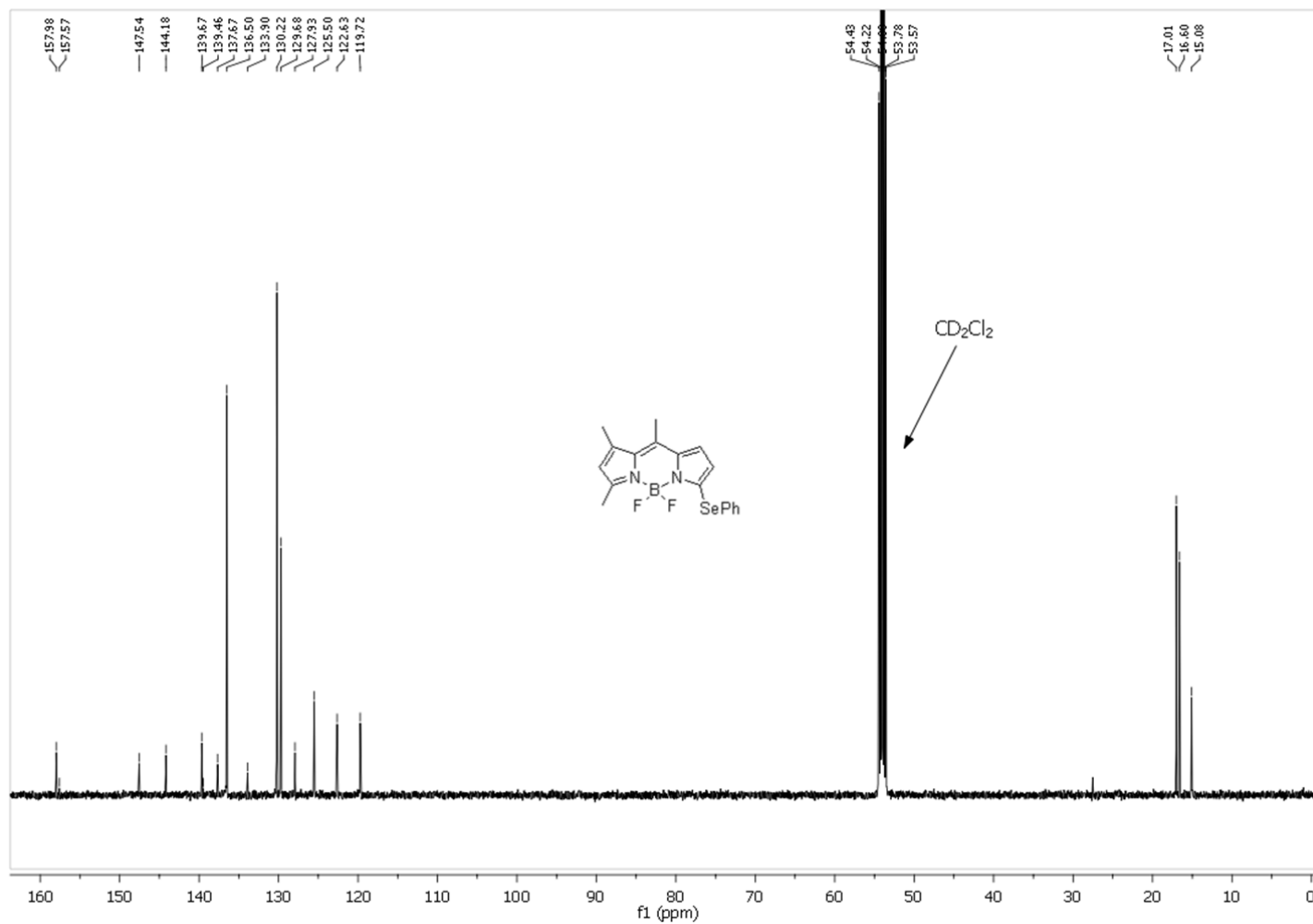


Figure S26:  $^1\text{H-NMR}$  of 3-phenyltellanyl-4,4-difluoro-5,7,8-trimethyl-4-bora-3a,4a-diaza-s-indacene (**3**) in acetone- $d_6$

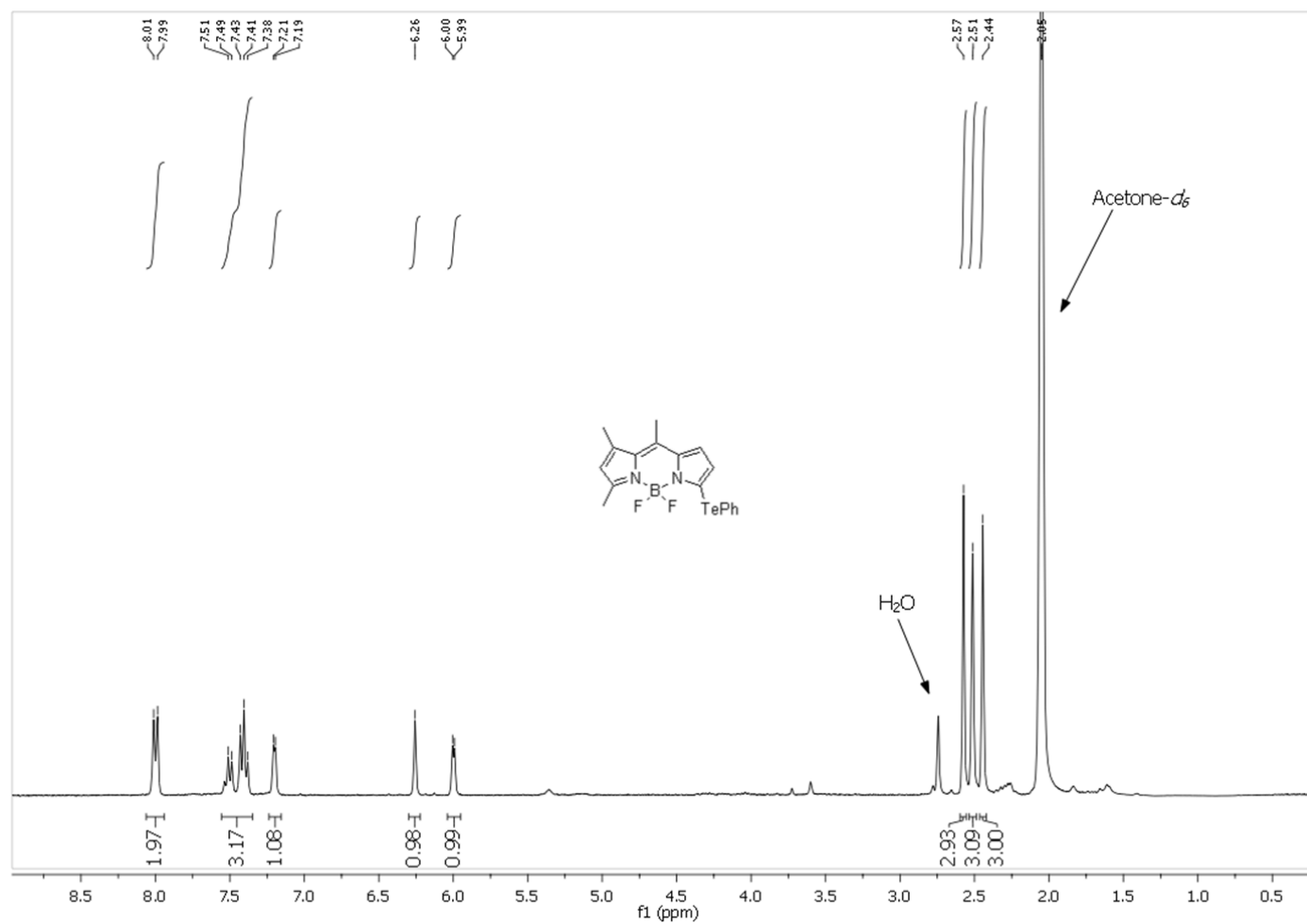


Figure S27:  $^{13}\text{C}$ -NMR of 3-phenyltellanyl-4,4-difluoro-5,7,8-trimethyl-4-bora-3a,4a-diaza-s-indacene (**3**) in acetone- $d_6$

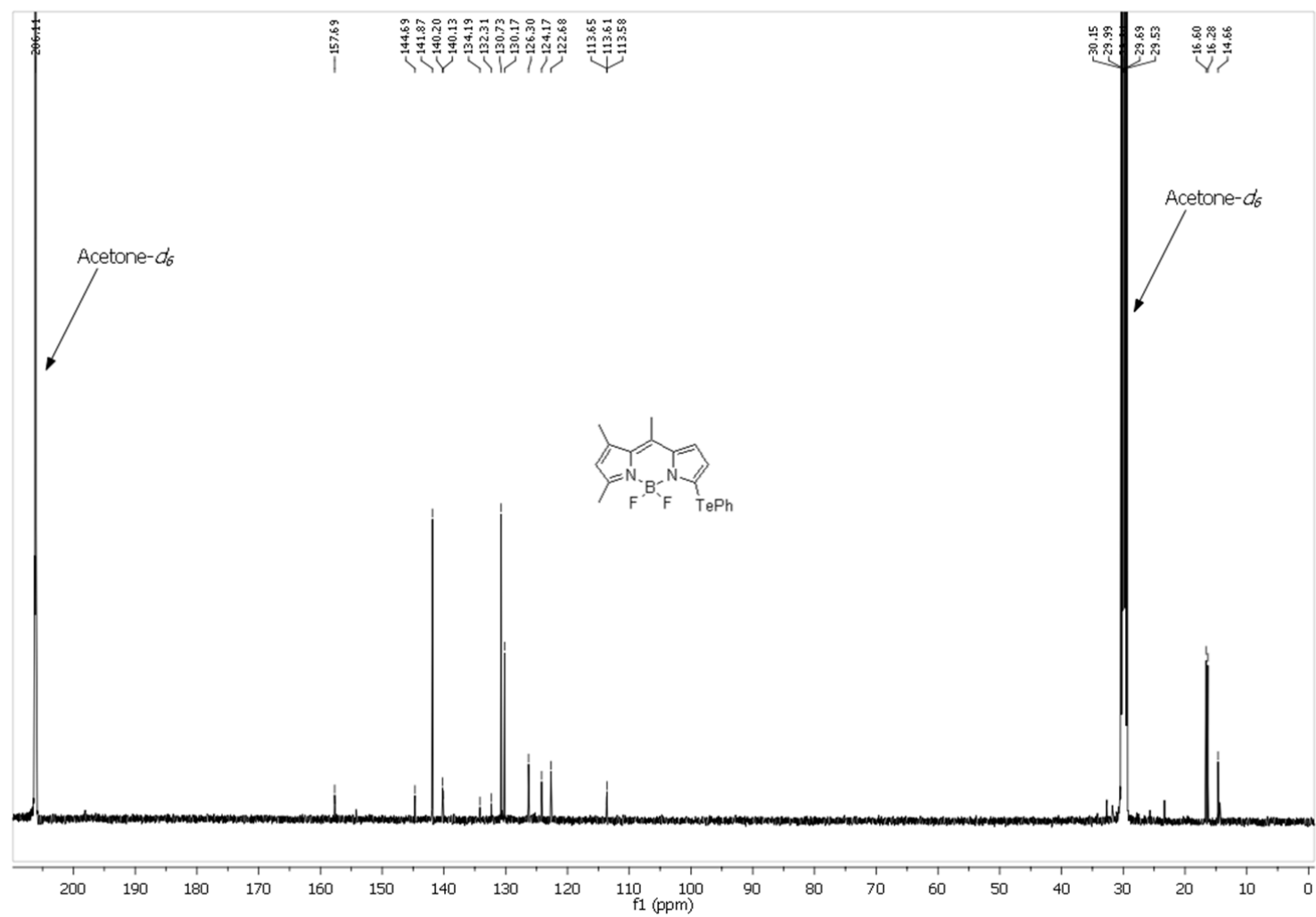


Figure S28:  $^1\text{H-NMR}$  of 4,4-difluoro-5,7,8-trimethyl-4-bora-3a,4a-diaza-*s*-indacene (**5**) in dichloromethane- $d_2$

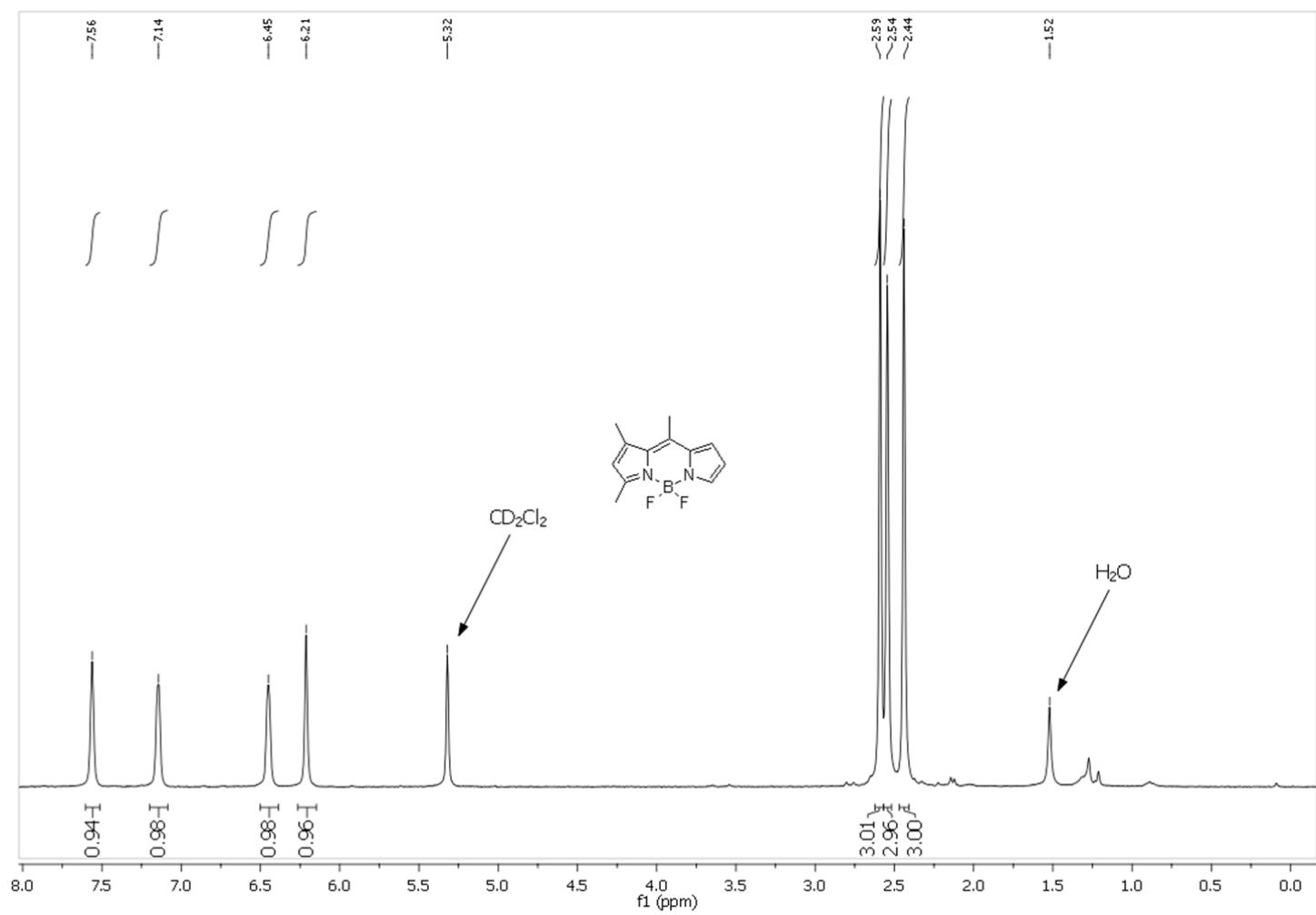
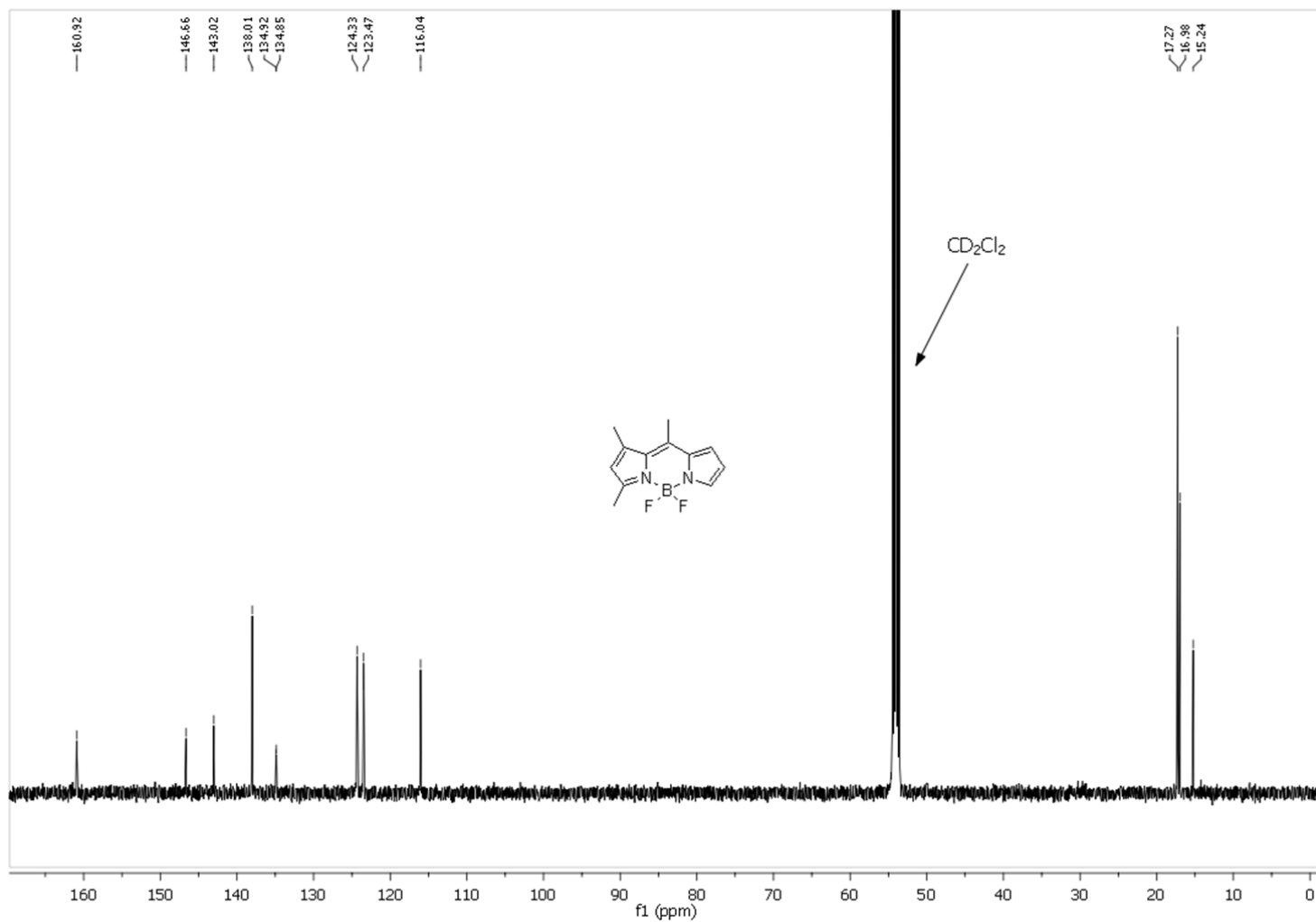


Figure S29:  $^{13}\text{C}$ -NMR of 4,4-difluoro-5,7,8-trimethyl-4-bora-3a,4a-diaza-*s*-indacene (**5**) in dichloromethane- $d_2$



## Determination of the Quantum Yield of Intersystem Crossing

**General Description.** The intersystem crossing quantum yields were determined using a previously published method.<sup>2</sup> It can be applied only in the region of the spectrum where the triplet state does not absorb. The amount of the triplet state formed at a given time after excitation corresponds to the amount of the ground state which was consumed via intersystem crossing (a ground state bleach signal). The magnitude of the ground state bleach signal ( $A^{\text{transient}}(\lambda)$ , a negative signal) equals to that of the ground state absorption ( $A(\lambda)$ , a positive signal) when the quantum yield of intersystem crossing ( $\Phi_{\text{isc}}$ ) equals to 1. Their sum equals to 0 (Eq. 1). If  $\Phi_{\text{isc}}$  equals to 0, no ground state bleach is observed (Eq. 2).

$$A(\lambda) + A^{\text{transient}}(\lambda) = 0 \quad \text{when } \Phi_{\text{isc}} = 1 \quad (\text{Eq. 1})$$

$$A(\lambda) + A^{\text{transient}}(\lambda) = A \quad \text{when } \Phi_{\text{isc}} = 0 \quad (\text{Eq. 2})$$

Equation 3 can be derived from Equations 1 and 2:

$$A(\lambda) \times \Phi_{\text{isc}} = -A(\lambda^{\text{transient}}) \quad (\text{Eq. 3})$$

The quantum yield of intersystem crossing can be computed by solving the integral from Equation 4 (the sum of residuals).

$$\int_{\lambda_1}^{\lambda_2} \left[ \frac{-A^{\text{transient}}(\lambda)}{\Phi_{\text{isc}}} - A(\lambda) \right] d\lambda = 0 \quad (\text{Eq. 4})$$

**A Step-by-step Procedure.** The absorption spectra of the ground state were measured using a transient spectroscopy apparatus (blank: a cuvette with solvent, no pump used) and recalculated with the molar absorption coefficient corresponding to the absorbance in a 10 mm cuvette (Figure S30). The transient spectra of **1** measured after 2–7 ns after the laser flash (the accumulation of the signal was set to 5 ns) are shown in Figure S31. The epsilon of the triplet was determined from the calibration of the setup by measuring the absorbance of the solution of the known concentration.

The absorption and transient spectra were averaged and the quantum yield of intersystem crossing was calculated by:

- 1) Multiplying the transient spectrum by  $-1$  which gives:  $(-1) \times A^{\text{transient}}(\lambda)$
- 2) Subtracting  $(-1) \times A^{\text{transient}}(\lambda)$  and the absorption spectrum  $A(\lambda)$  in the range where the triplet has no absorption (500–550 nm), which gives  $A^{\text{residuals}}(\lambda)$  (in the absolute values).
- 3) Integrating  $A^{\text{residuals}}(\lambda)$  in the range where the triplet does not absorb (500–550 nm for **1**), which gives the sum of the residuals.
- 4) Numerical minimizing the sum of residuals (Equation 4) by consecutive dividing  $(-1) \times A(\lambda^{\text{transient}})$  by a variable which ranges from 0 to 1, giving the quantum yield of intersystem crossing ( $\Phi_{\text{isc}}$ ). The whole process is graphically depicted in Figure S32.

**Figure S30:** Absorption spectra of **1** in aerated acetonitrile ( $c = 5.26 \times 10^{-6} \text{ mol dm}^{-3}$ ), recalculated for a 10 mm cuvette; repeated 11 times.

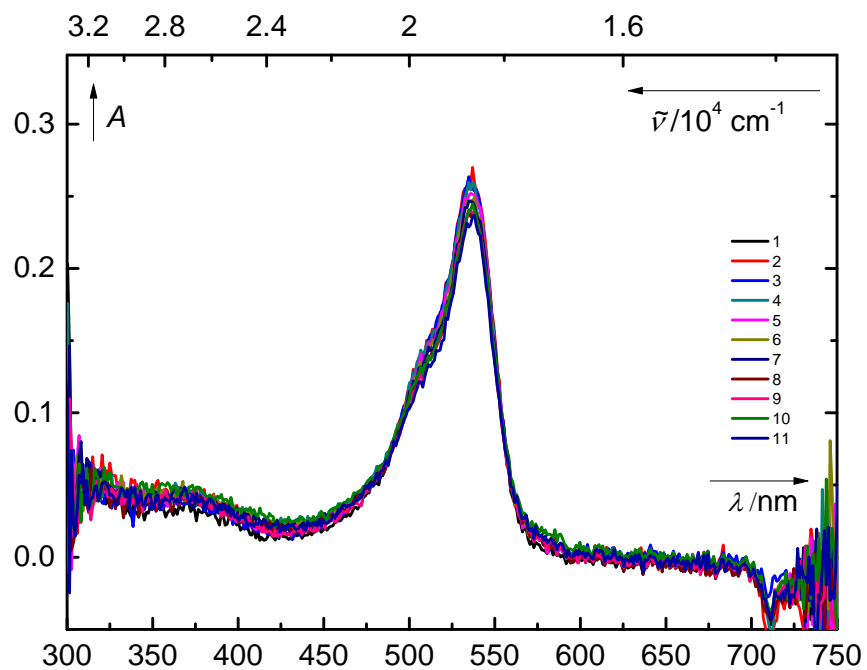


**Figure S31:** Transient spectra of **1** in aerated acetonitrile ( $c = 5.26 \times 10^{-6} \text{ mol dm}^{-3}$ ), 2–7 ns after the excitation, recalculated to epsilon; repeated 11 times.

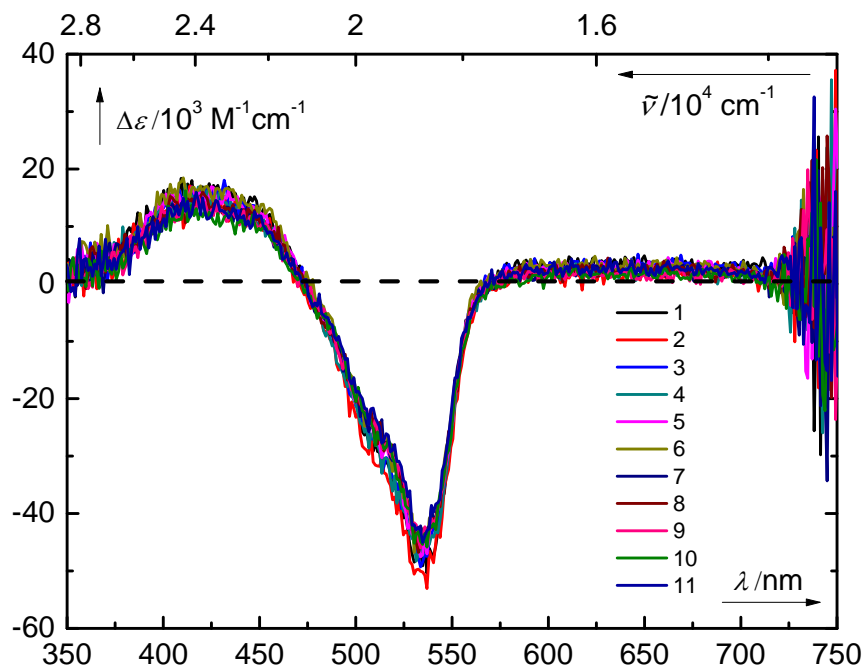


**Figure S32:** Graphical representation of the  $\Phi_{\text{isc}}$  calculation; the absorption spectrum:  $A(\lambda)$  (black line), the transient spectrum:  $A^{\text{transient}}(\lambda)$  (red line), the transient spectrum multiplied by  $-1$ :  $(-1) \times A^{\text{transient}}(\lambda)$  (blue line), the transient spectrum multiplied by  $-1$  and divided by  $\Phi_{\text{isc}}$ :  $\frac{-A^{\text{transient}}(\lambda)}{\Phi_{\text{isc}}}$  for a given value of  $\Phi_{\text{isc}} = 0.36$  (dark green line). The optimization (minimizing the sum of residuals vs.  $\Phi_{\text{isc}}$ ) for a model system is depicted in Figure S33.

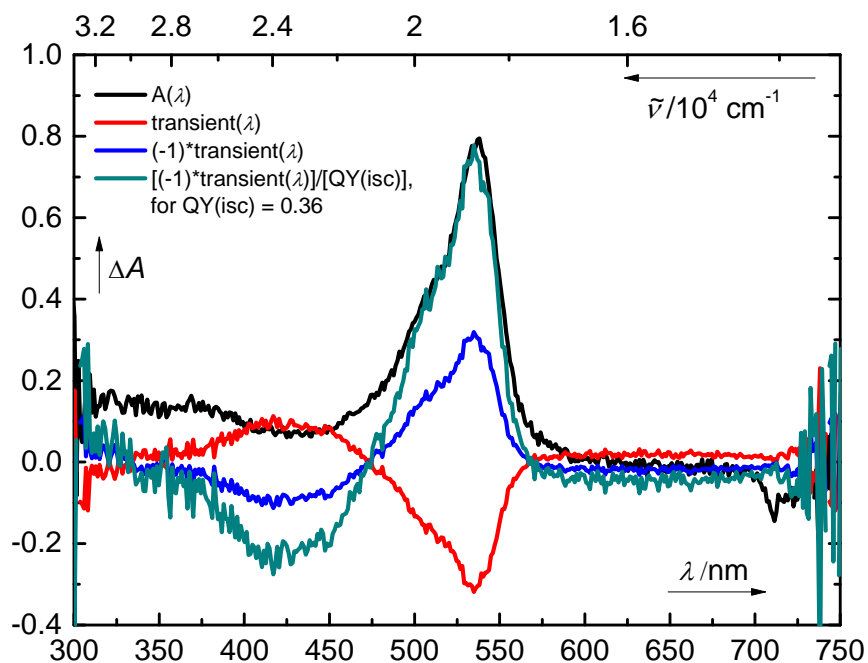
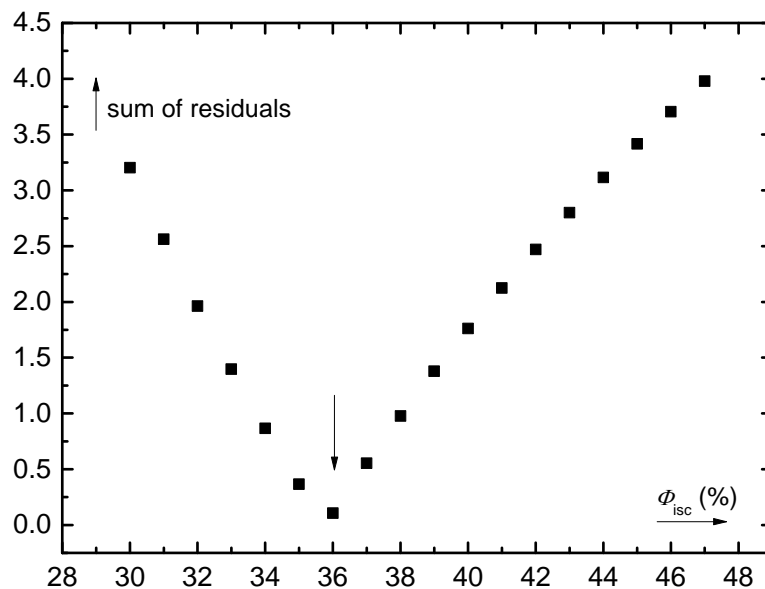


**Figure S33:** The result of optimization of  $\Phi_{\text{isc}}$  vs. the sum of residuals, a minimum value of the sum of residuals is at  $\Phi_{\text{isc}} = 0.36$ .



**Light Saturation Test.** The determination of the quantum yield of intersystem crossing by transient spectroscopy is based on an assumption that the excitation of the sample is quantitative, that is, all molecules in the sample are excited. We tested a dependence of the triplet signal intensity of **4** as a function of the laser energy (Figure S34), which was modulated by optical filters and by the setting of the laser amplification. The triplet absorption grew linearly up to  $\sim 140$  mJ, whereas at higher energies it leveled off. Therefore, the system became light saturated.

A linear dependence of the triplet state concentration (signal amplitude) of **4** at the energies of 25–150 mJ as well as the fact that the triplet-state lifetime does not depend on its analytical concentration (in range from  $10^{-4}$  to  $10^{-6}$  mol dm $^{-3}$ ) preclude self-quenching of the triplet by the ground-state **4**.

The representative decay traces of the triplet-state **4** excited by a laser at various energies are shown in Figure S35. The decay of the triplet state did not depend on the laser energy (and hence on the triplet concentration; Figure S36), and the decay rate constants at different laser intensities are equal to those in Table 3 in the manuscript. This indicates that there are no triplet-triplet interactions at given conditions which would influence the triplet-state quantum yield and its decay magnitude.

The light saturation conditions for compounds **1–3** ( $c = 1.5 \times 10^{-5}$  mol dm $^{-3}$ ) were reached at  $E \sim 100$  mJ at 532 nm, which is below the intensity used for our measurements (240 mJ).

**Figure S34:** Dependence of the initial intensity of triplet-triplet absorption of **4** at 420 nm ( $c = 4.5 \times 10^{-5} \text{ mol dm}^{-3}$  in acetonitrile, degassed), excited at 355 nm

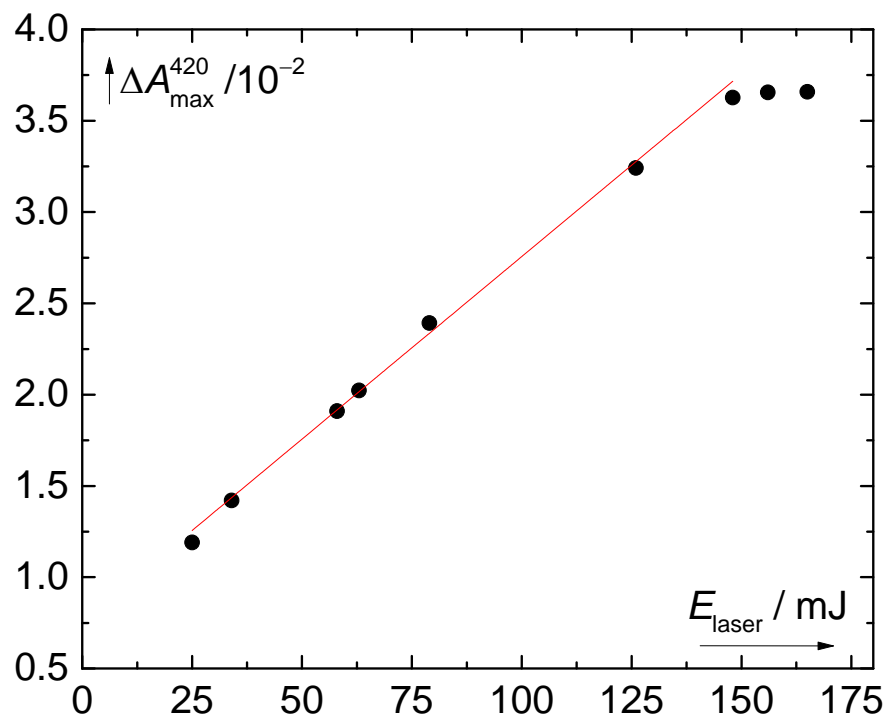


**Figure S35:** Decay traces of triplet state of **4** at 420 nm ( $c = 4.5 \times 10^{-5}$  mol dm<sup>-3</sup> in acetonitrile, degassed), excited at 355 nm by laser with different energies.

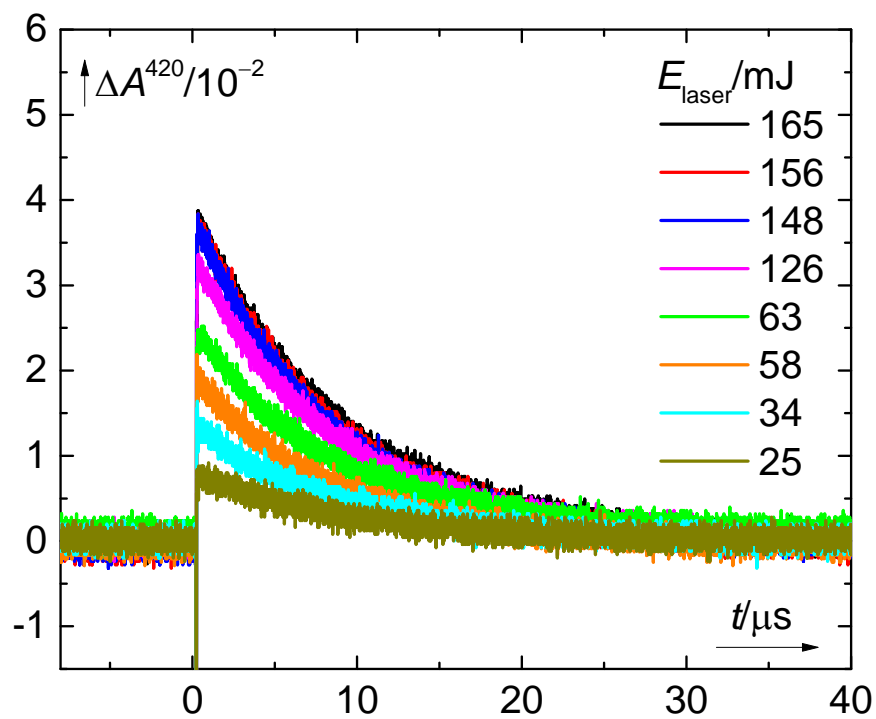
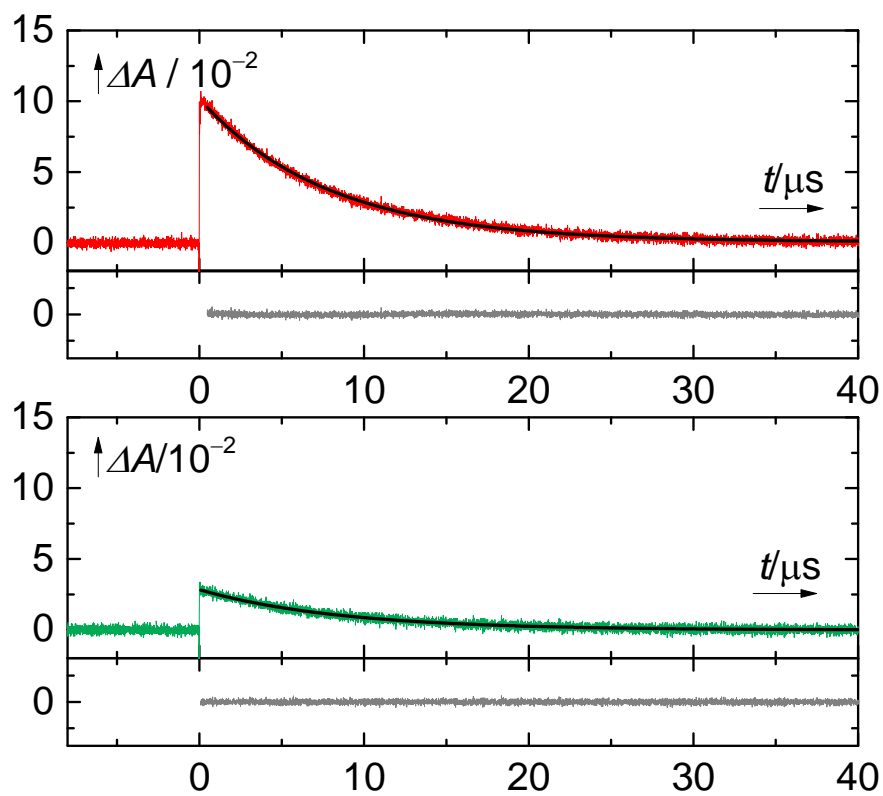


**Figure S36.** Representative kinetic traces and the residuals of a single-exponential fit of the signal for **4** excited at  $\lambda_{\text{exc}} = 355$  nm,  $E_{\text{laser}} = 156$  mJ (top, kinetic trace: red, exponential fit: black, sum of the residuals: gray) and  $E_{\text{laser}} = 25$  mJ (bottom, kinetic trace: green, exponential fit: black, sum of the residuals: gray) in degassed acetonitrile ( $c = 4.50 \times 10^{-5}$  mol dm $^{-3}$ ) obtained at  $\lambda = 420$  nm. The rate constant of decay in both cases equals to  $k_{\text{d}}^{\text{T}} = 1.4 \times 10^5$  s $^{-1}$ .

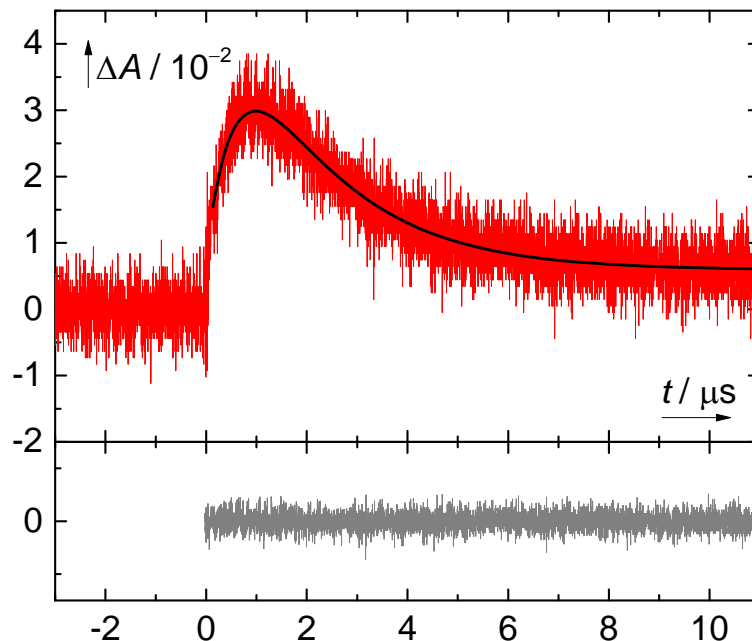


**Determination of the Quantum Yield of Intersystem Crossing Using a Reference Method.** Our method for the determination of the ISC quantum yields has also been compared with a well-established method reported by Das and coworkers based on sensitization of  $\beta$ -carotene,<sup>3</sup> which has also been utilized for several iodo-substituted aza-BODIPY chromophores.<sup>4</sup>

Therefore, the experimental procedure was adopted from Ramaiah and coworkers, who used  $[\text{Ru}(\text{bpy})_3](\text{BF}_4)_2$  as a standard triplet donor and  $\beta$ -carotene ( $c = 2.0 \times 10^{-4} \text{ mol dm}^{-3}$ ) as a triplet energy acceptor.<sup>4</sup> The triplet of  $\beta$ -carotene was monitored at 540 nm according to the original procedure.<sup>3</sup> The representative decay trace of  $\beta$ -carotene triplet sensitized by a triplet donor is shown in Figure S37. The direct excitation of  $\beta$ -carotene did not result in any significant triplet formation under used conditions.

The method is reliable under the assumption that energy transfer to  $\beta$ -carotene is 100% efficient.<sup>3</sup> The rate of the triplet decay of the triplet donor ( $[\text{Ru}(\text{bpy})_3](\text{BF}_4)_2$  or **4**) corresponded to the rate of increase of the  $\beta$ -carotene triplet, supporting a quantitative sensitization.

**Figure S37.** A representative kinetic trace and the residuals of a biexponential fit (rise and decay) of the signal for  $\beta$ -carotene ( $c = 2.0 \times 10^{-4} \text{ mol dm}^{-3}$ ) sensitized by  $[\text{Ru}(\text{bpy})_3](\text{BF}_4)_2$  ( $c = \sim 4.4 \times 10^{-5} \text{ mol dm}^{-3}$ ; degassed) in acetonitrile excited by a laser:  $E_{\text{pulse}} = 160 \text{ mJ}$  at  $\lambda_{\text{exc}} = 355 \text{ nm}$  (red: a kinetic trace; black: an exponential fit; gray: a sum of the residuals) obtained at  $\lambda = 540 \text{ nm}$ . The rate constants of the signal rise and decay are  $k_{\text{obs}} = (1.8 \pm 0.1) \times 10^6 \text{ s}^{-1}$  and  $k_{\text{decay}} = (5.3 \pm 0.2) \times 10^5 \text{ s}^{-1}$ , respectively.



The quantum yield of ISC was calculated from Equation 5 adapted from Das and coworkers:<sup>3</sup>

$$\Phi_{isc}^{BODIPY} = \Phi_{isc}^{ref} \frac{\Delta A^{BODIPY}}{\Delta A^{ref}} \frac{k_{obs}^{BODIPY}}{k_{obs}^{BODIPY} - k_0^{BODIPY}} \frac{k_{obs}^{ref} - k_0^{ref}}{k_{obs}^{ref}} \quad (\text{Eq. 5})$$

where  $\Phi_{isc}^{BODIPY}$  is the ISC quantum yield for a BODIPY derivative,  $\Phi_{isc}^{ref}$  is the intersystem crossing quantum yield for [Ru(bpy)<sub>3</sub>](BF<sub>4</sub>)<sub>2</sub>,  $\Delta A$  is the absorbance of the triplet state of  $\beta$ -carotene sensitized either by [Ru(bpy)<sub>3</sub>](BF<sub>4</sub>)<sub>2</sub> or by **4**,  $k_{obs}/s^{-1}$  is the pseudo-first-order rate constant for the decay of the donor triplets, and  $k_0/s^{-1}$  is the rate constant for the decay of the donor triplets in the absence of  $\beta$ -carotene.

The quantum yield of ISC of **4** was calculated using Equation 5 and the data in Table S1. We conclude that the reference method provided the same  $\Phi_{isc}$  value as the method used for this work (Table S1 and Table 3), which is much less experimentally demanding.

**Table S1.** Data for calculation of  $\Phi_{ISC}$  by the method according to Das and coworkers<sup>3</sup>

	[Ru(bpy) <sub>3</sub> ](BF <sub>4</sub> ) <sub>2</sub> <sup>a</sup>	<b>4</b> <sup>b</sup>
$k_0/s^{-1}$ <sup>c</sup>	$(9.9 \pm 0.1) \times 10^5$	$(1.4 \pm 0.1) \times 10^5$
$k_{obs}/s^{-1}$ <sup>d</sup>	$(1.8 \pm 0.1) \times 10^6$	$(1.10 \pm 0.03) \times 10^6$
$(k_{obs} - k_0)/s^{-1}$	$8.1 \times 10^5$	$9.5 \times 10^5$
$\Delta A$ <sup>e</sup>	$(3.1 \pm 0.1) \times 10^{-2}$	$(3.2 \pm 0.1) \times 10^{-2}$
$\Phi_{isc}$ <sup>f</sup>	1.0	<b>0.53 ± 0.01</b>

<sup>a</sup> An acetonitrile solution ( $c = \sim 4.4 \times 10^{-5}$  mol dm<sup>-3</sup>; degassed), excited by a laser:  $E_{pulse} = 160$  mJ at  $\lambda_{exc} = 355$  nm. <sup>b</sup> An acetonitrile solution ( $c = \sim 4.5 \times 10^{-5}$  mol dm<sup>-3</sup>; degassed) excited by a laser:  $E_{pulse} = 160$  mJ at  $\lambda_{exc} = 355$  nm. <sup>c</sup> The rate constant of decay of the excited triplet in the absence of a quencher obtained by a monoexponential fit. [Ru(bpy)<sub>3</sub>](BF<sub>4</sub>)<sub>2</sub>: the rate constants of decay at 365 nm or rise at 445 nm match the reported value  $(0.95 \pm 0.05) \times 10^6$ .<sup>5</sup> **4**: rate constant of the decay at 420 nm. <sup>d</sup> The pseudo-first-order rate constant for growth of the  $\beta$ -carotene triplet ( $\lambda = 540$  nm;  $c = 2.0 \times 10^{-4}$  mol dm<sup>-3</sup>) in the presence of a triplet donor ([Ru(bpy)<sub>3</sub>](BF<sub>4</sub>)<sub>2</sub> or **4**). <sup>e</sup> The maximum transient absorbance of the  $\beta$ -carotene triplet formed upon energy transfer from a triplet donor ([Ru(bpy)<sub>3</sub>](BF<sub>4</sub>)<sub>2</sub> or **4** monitored at 540 nm. <sup>f</sup> Quantum yield of ISC: [Ru(bpy)<sub>3</sub>](BF<sub>4</sub>)<sub>2</sub> from refs. 6 and 7; **4**: calculated according to Equation 5, averaged from 6 measurements.

## References

1. M. Kollmannsberger, T. Gareis, S. Heintz, J. Breu, J. Daub, Electrogenerated chemiluminescence and proton-dependent switching of fluorescence: Functionalized difluoroboradiaza-s-indacenes, *Angew. Chem. Int. Ed.*, 1997, **36**, 1333-1335.
2. R. Bonneau, I. Carmichael, G. L. Hug, Molar absorption coefficients of transient species in solution, *Pure Appl. Chem.*, 1991, **63**, 290-299.
3. C. V. Kumar, L. Qin, P. K. Das, Aromatic thioketone triplets and their quenching behaviour towards oxygen and di-*t*-butylnitroxy radical. A laser-flash-photolysis study, *J. Chem. Soc., Faraday Trans. 2*, 1984, **80**, 783-793.
4. N. Adarsh, M. Shanmugasundaram, R. R. Avirah, D. Ramaiah, Aza-BODIPY derivatives: Enhanced quantum yields of triplet excited states and the generation of singlet oxygen and their role as facile sustainable photooxygenation catalysts, *Chem. Eur. J.*, 2012, **18**, 12655-12662.
5. R. Bensasson, C. Salet, V. Balzani, Laser flash spectroscopy of tris(2,2'-bipyridine)ruthenium(II) in solution, *J. Am. Chem. Soc.*, 1976, **98**, 3722-3724.
6. F. Bolletta, M. Maestri, V. Balzani, Efficiency of the intersystem crossing from the lowest spin-allowed to the lowest spin-forbidden excited state of some chromium(III) and ruthenium(II) complexes, *J. Phys. Chem.*, 1976, **80**, 2499-2503.
7. J. N. Demas, D. G. Taylor, On the "intersystem crossing" yields in ruthenium(II) and osmium(II) photosensitizers, *Inorg. Chem.*, 1979, **18**, 3177-3179.